

University of California - Davis

UCD-98-2
hep-ph/9801417
January, 1998

SEARCHING FOR LOW-ENERGY SUPERSYMMETRY ^a

John F. Gunion

*Davis Institute for High Energy Physics,
Department of Physics,
University of California, Davis, CA 95616*

A review of supersymmetry theory and phenomenology is presented. Topics discussed include: gravity-mediated (SUGRA) and gauge-mediated (GMSB) supersymmetry breaking models; an overview of non-universal soft-supersymmetry-breaking masses and the resulting experimental implications; the phenomenology of and constraints on the possibility that a massive gluino is the lightest supersymmetric particle; current status of the phenomenology of the Higgs bosons of the minimal and next-to-minimal supersymmetric models; and, the signals for GMSB and/or R-parity-violating models coming from delayed decays of the lightest supersymmetric partner of the Standard Model particles.

1 Introduction

There are good reasons why supersymmetry (SUSY) is regarded by many as the most attractive candidate for the next level of physics beyond the Standard Model (SM). First, there are important aesthetic motivations for SUSY. i) It is the only non-trivial extension of the Lorentz group at the heart of quantum field theory. ii) If SUSY is formulated as a *local* symmetry, it becomes a supergravity (SUGRA) theory that reduces to general relativity in the appropriate limit. iii) SUSY appears in Superstrings. Second, although SUSY must be a broken symmetry since we have not yet observed supersymmetric particles, there are numerous indications that it will be realized at energies \lesssim few TeV. i) String theory solutions with a non-supersymmetric *ground* state are quite problematic. ii) SUSY solves the hierarchy problem, *e.g.* $m_{\text{Higgs}}^2 < (1 \text{ TeV})^2$ (as required to avoid a non-perturbative WW sector) via spin-1/2 loop cancellation of spin-0 loop quadratic divergences *provided* the masses (generically denoted by m_{SUSY}) of supersymmetric partners are \lesssim few TeV. iii) The minimal supersymmetric model (MSSM) leads to gauge coupling unification (at $M_U \sim \text{few} \times 10^{16} \text{ GeV}$) if $m_{\text{SUSY}} \lesssim 1 - 10 \text{ TeV}$. iv) In the MSSM, electroweak

^aTo appear in *Quantum Effects in the MSSM*, the Proceedings of the “International Workshop on Quantum Effects in the MSSM”, UAB, Barcelona, September 9–13, 1997, edited by J. Sola (World Scientific Publishing).

symmetry breaking (EWSB) can be a natural result of renormalization group evolution (RGE) if $m_t \sim 175$ GeV. v) In many cases, the lightest supersymmetric particle is a natural cold dark matter candidate.

However, there are many phenomenologically viable supersymmetry models. These and their experimental implications will be the primary subject of these lectures. The present review is an expanded version of Ref. [1]. Full referencing for the more introductory material can be found there. Here, I will include detailed referencing only for some of the relatively recent developments and for the collider phenomenology discussions.

2 The Minimal Supersymmetric Model

The minimal supersymmetric extension of the Standard Model consists of taking the Standard Model and adding the corresponding supersymmetric partners. The SM particles and corresponding sparticle mass eigenstates are listed below.

$$\begin{array}{cccc}
 [u, d, c, s, t, b] & g & \underbrace{W^\pm, H^\pm} & \underbrace{\gamma, Z, H_1^0, H_2^0} \\
 [\tilde{u}, \tilde{d}, \tilde{c}, \tilde{s}, \tilde{t}, \tilde{b}]_{L,R} & \tilde{g} & \tilde{\chi}_{1,2}^\pm & \tilde{\chi}_{1,2,3,4}^0
 \end{array}$$

In addition, the MSSM contains two hypercharge $Y = \pm 1$ Higgs doublets, which is the minimal structure for the Higgs sector of an anomaly-free supersymmetric extension of the Standard Model. The supersymmetric structure of the theory also requires (at least) two Higgs doublets to generate mass for both “up”-type and “down”-type quarks (and charged leptons). The physical Higgs mass eigenstates then comprise two CP-even Higgs bosons, h^0, H^0 (with $m_{h^0} \leq m_{H^0}$), a CP-odd Higgs boson, A^0 , and a charged Higgs pair, H^\pm .

In the MSSM, all renormalizable supersymmetric interactions consistent with (global) $B-L$ conservation are included. They are parameterized by:

- $SU(3) \times SU(2) \times U(1)$ gauge couplings, $g_3, g_2 \equiv g$, and $g_1 \equiv \sqrt{\frac{5}{3}} g'$;
- (complex) Higgs-quark Yukawa coupling matrices, $\mathbf{y}_u, \mathbf{y}_d$, and \mathbf{y}_e ; and
- a supersymmetric Higgs mass parameter, μ .

Since the MSSM is a model of three generations of quarks, leptons and their superpartners, $\mathbf{y}_u, \mathbf{y}_d$, and \mathbf{y}_e are complex 3×3 matrices. However, as discussed below, not all these degrees of freedom are physical.

As a consequence of $B-L$ invariance, the MSSM possesses a multiplicative R-parity invariance, such that all the ordinary Standard Model particles have

even R-parity, whereas the corresponding supersymmetric partners have odd R-parity.

In the MSSM, supersymmetry breaking is accomplished by including the most general renormalizable soft-supersymmetry-breaking terms consistent with the $SU(3) \times SU(2) \times U(1)$ gauge symmetry and R-parity conservation. These terms parameterize our ignorance of the fundamental mechanism of supersymmetry breaking. It is here where most of the new supersymmetric model parameters reside. As already noted, if supersymmetry is relevant for explaining the scale of electroweak interactions, then the mass parameters introduced by the soft-supersymmetry-breaking terms should be in the TeV range or below.

The soft-supersymmetry-breaking terms of the MSSM include:

- gaugino Majorana masses M_3 , M_2 , and M_1 , associated with the $SU(3)$, $SU(2)$, and $U(1)$ subgroups of the Standard Model;
- diagonal Higgs squared-mass terms, $m_{H_u}^2$, $m_{H_d}^2$;
- an off-diagonal Higgs squared-mass term, b (the “B”-term);
- (hermitian) squark and slepton squared-mass matrices, \mathbf{m}_Q^2 , \mathbf{m}_u^2 , \mathbf{m}_d^2 , \mathbf{m}_L^2 , \mathbf{m}_e^2 ;
- (complex) matrix A -parameters, \mathbf{a}_u , \mathbf{a}_d , \mathbf{a}_e , parameterizing Higgs-squark-squark and Higgs-slepton-slepton trilinear interactions.

As above, the quantities specified by boldface letters are 3×3 matrices (in generation space). Note that after minimizing the Higgs potential, one can trade in the three Higgs parameters $m_{H_u}^2$, $m_{H_d}^2$ and b for two neutral Higgs field vacuum expectation values v_u and v_d and one of the physical Higgs masses. Equivalently, one fixes $v^2 \equiv v_u^2 + v_d^2 = 4m_W^2/g^2 = (246 \text{ GeV})^2$ and introduces the parameter $\tan \beta \equiv v_u/v_d$.

There are many unphysical degrees of freedom among the MSSM parameters listed above. These can be eliminated by expressing interaction eigenstates in terms of the mass eigenstates, with an appropriate redefinition of the MSSM fields to remove unphysical phases. In the end, the MSSM possesses 124 truly independent parameters. Of these, 18 parameters correspond to Standard Model parameters (including the QCD vacuum angle θ_{QCD}), one corresponds to one of the Higgs sector masses (the analogue of the Standard Model Higgs mass), and 105 are genuinely new parameters of the model. These include: five real parameters and three CP-violating phases in the gauge/gaugino/Higgs/higgsino sector, 21 squark and slepton masses,

36 new real mixing angles to define the squark and slepton mass eigenstates and 40 new CP-violating phases that can appear in squark and slepton interactions. The most general R-parity conserving minimal supersymmetric extension of the Standard Model (without additional theoretical assumptions) will be denoted henceforth as MSSM-124.

MSSM-124 is phenomenologically viable only for very special domains in the full parameter space such that the following possible problems are absent: (i) non-conservation of the separate lepton numbers L_e , L_μ , and L_τ ; (ii) unsuppressed flavor-changing neutral currents (FCNC's); and (iii) new sources of CP-violation that are inconsistent with the experimental bounds.

There are a number of approaches for reducing the parameter freedom of MSSM-124 in such a way as to avoid these problems. There are two low-energy approaches. First, one can assume that the squark and slepton squared-mass matrices and the matrix A -parameters are proportional to the 3×3 unit matrix (horizontal universality). Alternatively, one can simply require that all the aforementioned matrices are flavor-diagonal in a basis where the quark and lepton mass matrices are diagonal (flavor alignment). In either case, L_e , L_μ and L_τ are separately conserved, while tree-level FCNC's are automatically absent. In both cases, the number of free parameters characterizing the MSSM is substantially less than 124. Both scenarios are phenomenologically viable, but there is no strong theoretical basis for either scenario.

In high-energy approaches, one treats the parameters of the MSSM as running parameters and imposes a particular structure on the soft-supersymmetry-breaking terms at a common high-energy scale [such as the GUT scale M_U or the reduced Planck scale $M_P = (8\pi G_N)^{-1/2} \sim 2.4 \times 10^{18}$ GeV]. Using the renormalization group equations, one can then derive the low-energy MSSM parameters. The initial conditions (at the appropriate high-energy scale) for the renormalization group equations depend on the mechanism by which supersymmetry breaking is communicated to the effective low-energy theory. One bonus of such an approach is that one of the diagonal Higgs squared-mass parameters is typically driven negative by renormalization group evolution. Thus, electroweak symmetry breaking is generated radiatively, and the resulting electroweak symmetry-breaking scale is intimately tied to the scale of low-energy supersymmetry breaking.

In the context of the MSSM, the high-energy approach is especially well-motivated given the fact that the MSSM particle content yields relatively exact gauge coupling unification (for sparticle masses $\lesssim 1 - 10$ TeV). If the gauge couplings become universal at M_U , then it is quite natural to suppose that the soft supersymmetry breaking parameters could also take a simple form at M_U . A number of points concerning gauge coupling unification should be

emphasized. a) Perturbative unification requires that the number of families in the $\lesssim 1$ TeV mass range be ≤ 4 . b) Unification occurs only if there are exactly 2 Higgs doublets, as in the MSSM, and possibly additional singlets, below M_U . Coupling unification in the presence of additional doublets, triplets and/or higher Higgs representations is only possible if appropriate additional matter fields with mass above 1–10 TeV and below M_U are introduced. c) The currently preferred smaller $\alpha_s(m_Z)$ values are most consistent with coupling unification if the ‘average’ sparticle mass m_{SUSY} is above 1 TeV. d) The fact that the predicted MSSM value of M_U is substantially below M_P may prove difficult to accommodate in specific string models.

To summarize, the word “minimal” in MSSM refers to the minimal particle spectrum and the associated R-parity invariance. The MSSM particle content must be supplemented by assumptions about the origin of supersymmetry-breaking that lie outside the low-energy domain of the model. The corresponding parameter freedom is bad if you want to know ahead of time exactly how to discover supersymmetry. Machine builders and experimentalists must be prepared for a wide range of possibilities as to how to see and fully explore SUSY. But, it is good in the sense that once the 105 new parameters of the MSSM have been experimentally determined you will have learned a great deal about the model. For example, in models where supersymmetry-breaking is mediated by gravitational interactions one can hope to discover an underlying organization for the 105 parameters (by evolving the low- E parameters up to M_U or M_P) that will define the GUT/String model visible sector properties. Different models lead to vastly different low- E parameters and expectations. The rest of the talk reviews some of the many possibilities discussed to date.

3 Constrained MSSM’s: mSUGRA and GMSB

In these theories, one posits a theory of dynamical supersymmetry-breaking (DSB), where the DSB occurs in a sector that is distinct from the fields of the MSSM. The supersymmetry-breaking inherent in the DSB sector is subsequently transmitted to the MSSM spectrum by some mechanism.

Two theoretical scenarios have been examined in detail: gravity-mediated and gauge-mediated supersymmetry breaking. In these approaches, supersymmetry is spontaneously broken, in which case a massless Goldstone fermion, the *goldstino*, arises. Its coupling to a particle and its superpartner is fixed by the supersymmetric Goldberger-Trieman relation:

$$\mathcal{L}_{\text{int}} = -\frac{1}{F} j^{\mu\alpha} \partial_\mu \tilde{G}_\alpha + \text{h.c.}, \quad (1)$$

where $j^{\mu\alpha}$ is the supercurrent, which depends bilinearly on all the fermion–

boson superpartner pairs of the theory and \tilde{G}_α is the spin-1/2 goldstino field (with spinor index α). \sqrt{F} is the scale at which supersymmetry-breaking occurs in the hidden sector (typically, $\sqrt{F} \gg m_Z$). When gravitational effects are included, the goldstino is “absorbed” by the *gravitino* ($\tilde{g}_{3/2}$), the spin-3/2 partner of the graviton. By this super-Higgs mechanism, the goldstino is removed from the physical spectrum and the gravitino acquires a mass ($m_{3/2}$). In models where the gravitino mass is generated at tree-level one finds

$$m_{3/2} = \frac{F}{\sqrt{3}M_{\text{P}}}. \quad (2)$$

The helicity $\pm\frac{1}{2}$ components of the gravitino behave approximately like the goldstino, whose couplings to particles and their superpartners are determined by Eq. (1). In contrast, the helicity $\pm\frac{3}{2}$ components of the gravitino couple with gravitational strength to particles and their superpartners, and thus can be neglected.

In many models, the DSB sector is comprised of fields that are completely neutral with respect to the Standard Model gauge group. In such cases, the DSB sector is also called the “hidden sector”. The fields of the MSSM are said to reside in the “visible sector”, and the model is constructed such that no renormalizable tree-level interactions exist between fields of the visible and hidden sectors. A third sector, the so-called “messenger sector”, is often employed in models to transmit the supersymmetry-breaking from the hidden sector to the visible sector. However, it is also possible to construct models in which the DSB sector is not strictly hidden and contains fields that are charged with respect to the Standard Model gauge group.

3.1 Gravity-mediated supersymmetry breaking

All particles feel the gravitational force. In particular, particles of the hidden sector and the visible sector can interact via the exchange of gravitons. Thus, supergravity (SUGRA) models provide a natural mechanism for transmitting the supersymmetry-breaking of the hidden sector to the particle spectrum of the MSSM. In models of *gravity-mediated* supersymmetry breaking, gravity is the messenger of supersymmetry-breaking. The resulting low-energy effective theory below the Planck scale consists of the unbroken MSSM plus all possible soft-supersymmetry-breaking terms.

For example, the gaugino masses could arise primarily from an effective Lagrangian term of the form

$$\mathcal{L} = \int d^2\theta W_a W_b \frac{\hat{\Phi}_{ab}}{M_{\text{P}}} + h.c. \sim \frac{\langle F_\Phi \rangle_{ab}}{M_{\text{P}}} \lambda_a \lambda_b, \quad (3)$$

where the $\lambda_{a,b}$ ($a, b = 1, 2, 3$) are the gaugino fields and F_Φ is the auxiliary component of a hidden sector superfield $\hat{\Phi}$ that appears linearly in the gauge kinetic function. The scale M_P appears in the denominator when communication between the hidden sector and the MSSM sector is via gravitational interactions. F in the previous section should be identified with $\langle F_\Phi \rangle$. From Eq. (3) we see that in order for gauginos to have mass $\mathcal{O}(m_W)$, $\sqrt{F} \sim \sqrt{m_W M_P} \sim 10^{10}$ GeV is required. Such a large \sqrt{F} value implies that the gravitino mass, Eq. (2), is larger than the mass of the lightest neutralino, $\tilde{\chi}_1^0$. Since the gravitino is also *very* weakly interacting when \sqrt{F} is large, Eq. (1), it becomes phenomenologically irrelevant.

In a *minimal* supergravity (mSUGRA) framework, the soft-supersymmetry breaking parameters at the Planck or GUT scale take a particularly simple form. First, the gaugino mass parameters as well as the gauge couplings are presumed to unify at some scale M_X ($= M_U$ or M_P ?):

$$M_1(M_X) = M_2(M_X) = M_3(M_X) \equiv m_{1/2}. \quad (4)$$

[For example, in the context of Eq. (3), the field $\hat{\Phi}$ of the hidden sector would be presumed to be a flavor singlet, implying $\langle F_\Phi \rangle \propto c\delta_{ab}$.] Eq. (4) implies that the low-energy gaugino mass parameters satisfy:

$$M_3 = \frac{g_3^2}{g_2^2} M_2 \simeq 3.5 M_2, \quad M_1 = \frac{5}{3} \tan^2 \theta_W M_2 \simeq 0.5 M_2. \quad (5)$$

Second, the scalar squared masses and the A -parameters are taken to be flavor-diagonal and universal:

$$\begin{aligned} \mathbf{m}_Q^2(M_P) &= \mathbf{m}_U^2(M_P) = \mathbf{m}_D^2(M_P) = \mathbf{m}_L^2(M_P) = \mathbf{m}_E^2(M_P) = m_0^2 \mathbf{1}, \\ m_{H_u}^2(M_P) &= m_{H_d}^2(M_P) = m_0^2, \\ \mathbf{a}_f(M_P) &= A_0 \mathbf{y}_f(M_P), \quad \mathbf{f} = \mathbf{u}, \mathbf{d}, \mathbf{e}, \end{aligned} \quad (6)$$

where $\mathbf{1}$ is the 3×3 identity matrix in generation space, and the \mathbf{y}_f are the Higgs-fermion Yukawa coupling matrices. Finally, μ , b and the gaugino mass parameters are assumed (rather arbitrarily) to be initially real at the high scale.

It is easy to count the number of free parameters of mSUGRA. The low-energy values of the MSSM parameters are determined by the MSSM renormalization group equations and the above initial conditions [Eqs. (4) and (6)]. Thus, the mSUGRA model is fixed by the following parameters: 18 Standard Model parameters (excluding the Higgs mass), m_0 , $m_{1/2}$, A_0 , $\tan \beta$, and $\text{sgn}(\mu)$ for a total of 23 parameters. This result was obtained by trading in

the parameters b and μ^2 for v^2 (which is counted as one of the 18 Standard Model parameters) and $\tan\beta$. In this procedure the sign of μ is not fixed, and so it remains an independent degree of freedom. The requirement of radiative electroweak symmetry breaking imposes an additional constraint on the possible range of the mSUGRA parameters. In particular, one finds that $1 \lesssim \tan\beta \lesssim m_t/m_b$. In principle, the mass of the gravitino, $m_{3/2}$ (or equivalently, \sqrt{F}), is an additional independent parameter. But, as discussed above, the gravitino does not play any role in mSUGRA phenomenology.

Clearly, mSUGRA is much more predictive than MSSM-124. In particular, one has only four genuinely new parameters beyond the Standard Model (plus a two-fold ambiguity corresponding to the sign of μ), from which one can predict the entire MSSM spectrum and its interactions. It will be convenient to reference a number of specific mSUGRA parameter sets. The first is the ‘Standard’ Snowmass96 Point, defined by $m_0 = 200$ GeV, $m_{1/2} = 100$ GeV, $A_0 = 0$, $\tan\beta = 2$, $\mu < 0$. Other interesting parameter sets include the String/SUGRA motivated No-Scale ($m_{1/2} \neq 0$, $m_0 = A_0 = 0$) and Dilaton or Dilaton-Like ($m_{1/2} = -A_0 = \sqrt{3}m_0$) models. The latter are perhaps particularly worthy of considering since to deviate significantly from dilaton-like boundary conditions in Calabi-Yau and Orbifold models requires that supersymmetry breaking be overwhelmingly dominated by moduli fields other than the dilaton ($\sin\theta_{\text{goldstino}} \ll 1$). This is because in the absence of loop corrections the dilaton boundary conditions apply with $m_{1/2} = m_{3/2} \sin\theta_{\text{goldstino}}$ and it is only when $m_{3/2} \sin\theta_{\text{goldstino}}$ is small compared to loop corrections that we can move away from dilaton boundary conditions. Vacuum stability against color breaking, might be a problem for this model, but it currently appears that metastability and/or non-perturbative effects can cure the apparent difficulty. In both the no-scale and dilaton cases, two parameters (usually chosen to be $m_{1/2}$ and $\tan\beta$) and the sign of μ are sufficient to completely specify the model.

The mSUGRA initial conditions of Eq. (6) correspond to a minimal SUGRA framework (specifically, the kinetic energy terms for the gauge and matter fields are assumed to take a minimal canonical form). Since there is no theoretical principle that enforces such a minimal structure, perturbations of the mSUGRA initial conditions consistent with phenomenology (*e.g.* avoiding the generation of dangerous FCNC’s) have been considered [2,3]. For example, one can introduce separate mass scales for the Higgs and squark/slepton soft-supersymmetry-breaking masses. One can also introduce non-universal scalar masses, but restrict the size of the non-universal terms to be consistent with phenomenology. Finally, gaugino mass unification is *not* required by either theory or phenomenological constraints. Specific examples of all these devia-

tions arise in string-inspired models [4]. Models which violate the mSUGRA initial conditions that appear to be of particular interest include:

- Strange-event-motivated models. For example, the phenomenology of $M_1 \simeq M_2$ [in contrast to $M_1 \simeq 0.5M_2$ predicted by Eq. (5)] has recently been advocated [5] in order to provide a possible explanation for the famous CDF $ee\gamma\gamma$ event.
- Scenarios with $M_2 < M_1$, resulting in the $\tilde{\chi}_1^0$ and $\tilde{\chi}_1^\pm$ both being wino-like and nearly degenerate in mass.
- The light gluino scenario, in which the M_i are set to zero.
- Scenarios in which non-universality for the M_i is such that the gluino has substantial mass, but is the lightest of the gauginos.

Non-Universal Gaugino Masses

Non-universal gaugino masses are particularly interesting from a phenomenological viewpoint. Models with substantial theoretical motivation include the following.

- The O-II Orbifold String model with all matter fields in the $n = -1$ untwisted sector, and supersymmetry breaking dominated by the overall size modulus (as opposed to the dilaton). The phenomenology of this model is explored in Ref. [6].

This is the only known string-based model in which the limit of pure modulus (no dilaton) supersymmetry breaking is possible without charge and/or color breaking. The gaugino masses arise from 1-loop terms generic to any theory; the resulting M_U boundary conditions take the form

$$M_a^0 \sim \sqrt{3}m_{3/2}[-(b_a + \delta_{GS})K\eta], \quad m_0^2 = m_{3/2}^2[-\delta_{GS}K'], \quad A_0 = 0, \quad (7)$$

where the b_a are the gauge RGE coefficients ($b_3 = 3, b_2 = -1, b_1 = -33/5$), δ_{GS} is the Green-Schwarz mixing parameter (a negative integer in the O-II model, with $\delta_{GS} = -3, -4, -5$ preferred), and $\eta = \pm 1$. The one-loop estimates of $K = 4.6 \times 10^{-4}$ and $K' = 10^{-3}$ imply $m_{\tilde{\ell}}, m_{\tilde{q}} \gg M_a$. We emphasize that the above relation of M_a to b_a, δ_{GS} that arises at one-loop is more general than the O-II model; in particular, it is likely to survive non-perturbative corrections. However, the relation between K and K' is model-dependent.

- F -term breaking with $F \neq \text{SU}(5)$ singlet. The phenomenology of these models is discussed in Ref. [3].

F_Φ	M_U			m_Z		
	M_3	M_2	M_1	M_3	M_2	M_1
1	1	1	1	~ 6	~ 2	~ 1
24	2	-3	-1	~ 12	~ -6	~ -1
75	1	3	-5	~ 6	~ 6	~ -5
200	1	2	10	~ 6	~ 4	~ 10
$O-II$ $\delta_{GS} = -4$	1	5	$\frac{53}{5}$	~ 6	~ 10	$\sim \frac{53}{5}$

Table 1: M_a at M_U and m_Z for the four F_Φ irreducible representations and in the O-II model with $\delta_{GS} \sim -4$.

In these models, it is supposed that the hidden sector is not completely hidden; it contains some fields with ordinary quantum numbers. In particular, referring to Eq. (3), suppose that $\hat{\Phi}$ is not a singlet field. In general, it is only required that

$$\hat{\Phi}, F_\Phi \in (\mathbf{24} \times \mathbf{24})_{\text{symmetric}} = \mathbf{1} \oplus \mathbf{24} \oplus \mathbf{75} \oplus \mathbf{200}. \quad (8)$$

For higher representations, only F_Φ components that are ‘neutral’ with respect to the SU(3), SU(2), U(1) gauge groups can acquire a vev if these groups are to remain unbroken after supersymmetry breaking. The result is that $\langle F_\Phi \rangle_{ab} = c_a \delta_{ab}$, with c_a depending on the representation (an arbitrary superposition of representations also being possible). The relative gaugino masses are tabulated in Table 1.

To obtain a first appreciation for the phenomenological implications we give in Table 2 the low-energy gaugino masses for these cases, assuming the Snowmass96 point $m_{\tilde{g}} \sim 285$ GeV value for the gluino mass. The fact that $m_{\tilde{\chi}_1^0} \sim \min(M_1, M_2)$ and $m_{\tilde{\chi}_1^\pm} \sim M_2$ (after mass matrix diagonalization) implies that in the **200** and O-II models (which have $M_2 \lesssim M_1$) $m_{\tilde{\chi}_1^\pm} \simeq m_{\tilde{\chi}_1^0}$ (and both are winos). Of course, the relative masses depend upon $\tan\beta$ as illustrated in Ref. [3]. In the O-II model, the dependence of the ino masses on δ_{GS} , illustrated in Fig. 1, is also quite illuminating. Note that for a narrow range of δ_{GS} (near the theoretically preferred values), the gluino will be the LSP! The detailed phenomenological implications of these results will be outlined later.

- The light-gluino scenario.

In this scenario [7], the soft-supersymmetry-breaking gaugino masses M_i are taken to be zero at tree-level and only arise at one-loop. The result is that $\tilde{\chi}_1^0 \sim$

	1	24	75	200	$O-II$ $\delta_{GS} = -4.7$
$m_{\tilde{g}}$	285	285	287	288	313
$m_{\tilde{u}_R}$	302	301	326	394	big
$m_{\tilde{t}_1}$	255	257	235	292	big
$m_{\tilde{t}_2}$	315	321	351	325	big
$m_{\tilde{b}_L}$	266	276	307	264	big
$m_{\tilde{b}_R}$	303	303	309	328	big
$m_{\tilde{\ell}_R}$	207	204	280	437	big
$m_{\tilde{\ell}_L}$	216	229	305	313	big
$m_{\tilde{\chi}_1^0}$	44.5	12.2	189	174.17	303.09
$m_{\tilde{\chi}_2^0}$	97.0	93.6	235	298	337
$m_{\tilde{\chi}_1^\pm}$	96.4	90.0	240	174.57	303.33
$m_{\tilde{\chi}_2^\pm}$	275	283	291	311	big
m_{h^0}	67	67	68	70	82

Table 2: Sparticle masses for the Snowmass96 comparison point.

$\tilde{\gamma}$ with $m_{\tilde{\chi}_1^0} \sim 0.1 - 1.5$ GeV (from one-loop squark-quark and wino/higgsino-Higgs/vector boson diagrams) and $m_{\tilde{g}} \sim 10 - 600$ MeV (from one-loop squark-quark diagrams). The lightest supersymmetric particle will be the lightest ‘R-hadron’, which is likely to be the $R^0 = \tilde{g}g$ with mass of order 1.5 GeV. It is claimed [8] that this model is highly disfavored on the basis of $2j$ and $4j$ event shapes in Z decay, which, for example, constrain the running of α_s via $b = (11/6)C_A/C_F - (2/3)n_f T_F/C_F$. A light \tilde{g} acts like 3 new flavors, increasing n_f from ~ 5 to ~ 8 . Another immutable prediction of the model is that $m_{\tilde{\chi}_1^\pm} \leq m_W$. Thus, LEP-2 running at $\sqrt{s} \sim 190$ GeV should soon find evidence for the chargino (despite the possibly complicated decay patterns) or the model will be ruled out. It is important to note that these searches do not constrain the possibility noted in the previous item of a heavy gluino-LSP.

3.2 Gauge-mediated supersymmetry-breaking

The theory of gauge-mediated supersymmetry breaking (GMSB) [9] posits that supersymmetry breaking is transmitted to the MSSM via gauge forces. Two model-building approaches have been recently explored in the literature. First, in hidden-sector models, the GMSB model consists of three distinct sectors: a hidden (DSB) sector where supersymmetry is broken, a ‘messenger’

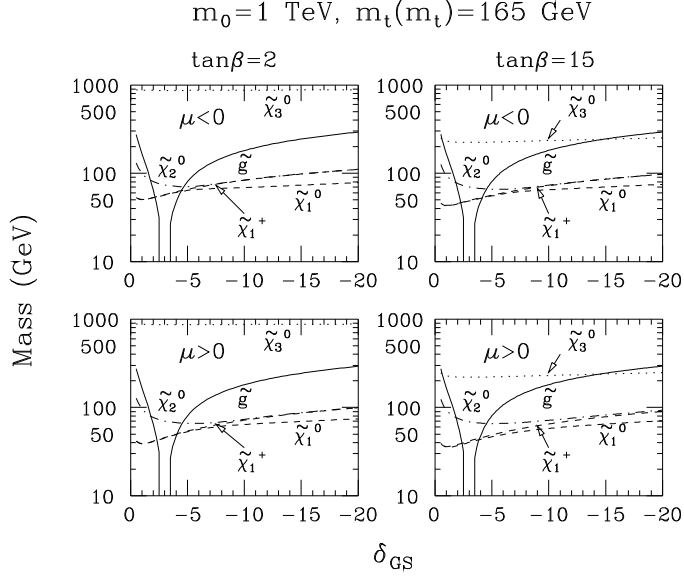


Figure 1: O-II model predictions for $m_{\tilde{\chi}_1^0}$, $m_{\tilde{\chi}_2^0}$, $m_{\tilde{\chi}_3^0}$, $m_{\tilde{\chi}_1^+}$, and $m_{\tilde{g}}$ as functions of δ_{GS} at $\tan\beta = 2, 15$ for $\mu > 0$ and $\mu < 0$.

sector consisting of messenger fields with $SU(3) \times SU(2) \times U(1)$ quantum numbers, and a sector containing the fields of the MSSM [10]. The direct coupling of the messengers to the hidden sector generates a supersymmetry-breaking spectrum in the messenger sector. Second, in models of “direct gauge mediation” (sometimes called direct-transmission models) [11], the GMSB model consists only of two distinct sectors: the DSB sector (which also contains the messenger fields) and the sector of MSSM fields. In both classes of models, supersymmetry-breaking is transmitted to the MSSM via $SU(3) \times SU(2) \times U(1)$ gauge interactions between messenger fields and the MSSM fields. In particular, supersymmetry-breaking masses for the gauginos and squared-masses for the squarks and sleptons arise, respectively, from one-loop and two-loop diagrams involving the virtual exchange of messenger fields.

In simple hidden-sector GMSB models, gaugino masses have the same relative values as if they were unified as specified in Eq. (4) (with M_X of order M_U) even though the actual initial conditions are set at scale M_m . For example, in the minimal model where supersymmetry-breaking effects in the messenger sector are small compared to M_m , one finds the following result for

the gaugino Majorana mass terms [10]:

$$M_i(M_m) = k_i N_m g \left(\frac{\Lambda}{M_m} \right) \frac{\alpha_i(M_m)}{4\pi} \Lambda, \quad (9)$$

where $k_2 = k_3 = 1$, $k_1 = 5/3$, and N_m denotes the effective number of messengers in the messenger sector — $N_m \leq 4$ is required to avoid Landau poles. Λ is an effective mass scale that depends on the details of the GMSB model. In addition, scalar masses are expected to be flavor-independent since the mediating gauge forces are flavor-blind. In the simplest hidden-sector models they take the form:

$$m_i^2(M_m) = 2\Lambda^2 N_m f \left(\frac{\Lambda}{M_m} \right) \sum_{i=1}^3 c_i \left(\frac{\alpha_i(M_m)}{4\pi} \right)^2 \quad (10)$$

with $c_3 = 4/3$ (triplets) $c_2 = 3/4$ (weak doublets), and $c_1 = \frac{5}{3} \left(\frac{Y}{2} \right)^2$ in the normalization where $Y/2 = Q - T_3$. Thus, degeneracy among families is broken only by effects of order quark or lepton Yukawa couplings. In Eqs. (9) and (10), $M_m/\Lambda > 1$ is required to avoid negative mass-squared for bosonic members of the messenger sector; $M_m/\Lambda \geq 1.1$ is preferred to avoid fine-tuning, for which $f(\Lambda/M_m) \simeq 1$ and $1 \leq g(\Lambda/M_m) \leq 1.23$. For $M_m/\Lambda \geq 2$, $1 \leq g(\Lambda/M_m) \leq 1.045$. In the approximation $g = f = 1$, one finds (at tree-level) $m_{\tilde{q}} : m_{\tilde{\ell}_L} : m_{\tilde{\ell}_R} : M_1 = 11.6 : 2.5 : 1.1 : \sqrt{N_m}$,^b which implies that the next to lightest supersymmetric particle (the goldstino being the lightest) is the $\tilde{\chi}_1^0 \simeq \tilde{B}$ for $N_m = 1$ or the $\tilde{\ell}_R$'s for $N_m \geq 2$. Note that supersymmetric scalar and gaugino states with the same color quantum numbers have masses of roughly the same magnitude.

In order that all superpartner masses be $\lesssim 1$ TeV, it follows [*e.g.*, from Eq. (9)] that $\Lambda \lesssim 100$ TeV. For example, for $N_m = 1$

$$\Lambda \sim 80 \text{ TeV} \left(\frac{M_1}{100 \text{ GeV}} \right), \quad (11)$$

where M_1 is the low-energy value of the U(1)-gaugino soft-supersymmetry-breaking mass and the gluino mass is $m_{\tilde{g}} \sim 7M_1$. The masses of various sparticles in the case of $N_m = 1$ are plotted as a function of Λ (taking $f = g = 1$) in Fig. 2.

^bEvolution corrections [12] in going from scale M_m to the $\lesssim 1$ TeV scale do not destroy this ordering unless M_m is very large, although they do affect the precise numerical ratios.

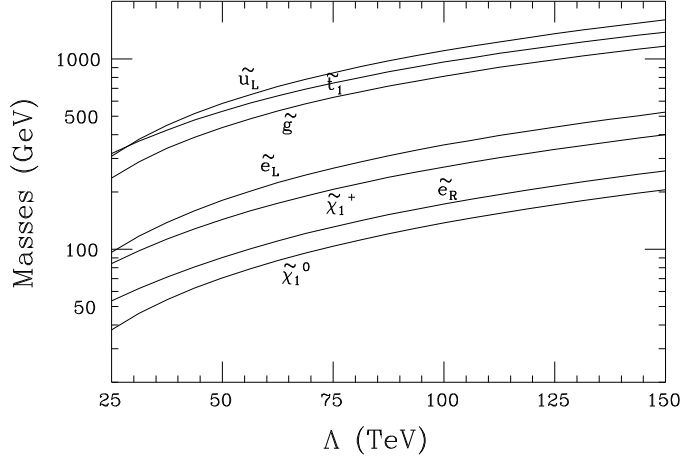


Figure 2: $m_{\tilde{\chi}_1^0}$, $m_{\tilde{\chi}_1^+}$, $m_{\tilde{e}_R}$, $m_{\tilde{e}_L}$, $m_{\tilde{g}}$, $m_{\tilde{t}_1}$ and $m_{\tilde{u}_L}$ as functions of Λ in the $N_m = 1$ GMSB scenario, taking $f = g = 1$ and $M_m = 1.1\Lambda$.

As for the other parameters of low-energy supersymmetry, the A -parameters are suppressed, while the generation of μ and b is quite model-dependent (and lies somewhat outside the standard ansatz of gauge-mediated supersymmetry breaking). The initial conditions for the soft-supersymmetry-breaking running parameters are fixed at M_m , which characterizes the average mass of messenger particles. In principle, M_m can lie anywhere between (roughly) Λ and 10^{16} GeV (in models with larger values of M_m , supergravity-mediated effects would dominate the gauge-mediated effects). Thus, the minimal GMSB model [13] contains 18 Standard Model parameters, Λ , $\tan \beta$ and $\arg(\mu)$ [after trading in b and $|\mu|^2$ for v and $\tan \beta$]. There is also a weak logarithmic dependence on M_m , which enters through renormalization group running. We thus end up with 22 free parameters. Clearly, the minimal GMSB approach is even more predictive than the mSUGRA model.

When the GMSB approach is extended to incorporate gravitational phenomena, supergravity effects will also contribute to supersymmetry breaking. However, in models of gauge-mediated supersymmetry breaking, one usually chooses the model parameters in such a way that the virtual messenger exchange diagrams dominate the effects of the direct gravitational interactions between the hidden and visible sectors. However, of critical importance is the fact that the super-Higgs effect becomes operative, and the gravitino absorbs the goldstino and becomes massive. Using Eq. (2), it is convenient to rewrite

the formula for the gravitino mass as follows:

$$m_{3/2} = \frac{F}{\sqrt{3}M_{\text{P}}} \sim 2.5 \left(\frac{\sqrt{F}}{100 \text{ TeV}} \right)^2 \text{ eV}. \quad (12)$$

The scale of supersymmetry breaking, \sqrt{F} , is a very crucial parameter in GMSB models. It is highly model-dependent. In hidden-sector models, values of $\sqrt{F} \gtrsim 10^3\text{--}10^4$ TeV are required in order to generate sufficiently large supersymmetry-breaking in the sector of MSSM fields [14,15,16]. In particular, one can derive [14,16] the approximate inequality

$$\left(\frac{\sqrt{F}}{2000 \text{ TeV}} \right) \geq f \left(\frac{m_{\tilde{\ell}_R}}{100 \text{ GeV}} \right) \left(\frac{1}{27.5\sqrt{N_m}} \right), \quad (13)$$

where $f \sim \left(\frac{g_m^2}{16\pi^2} \right)^{-2} \sim 2.5 \times 10^4 / g_m^4$, with g_m being the coupling of the gauge group responsible for communicating (via two-loop diagrams) supersymmetry breaking from the hidden sector to the messenger sector. Perturbativity would require $g_m \lesssim 1$. For $m_{\tilde{\ell}_R} \geq 45$ GeV (the rough LEP limit) and $f = 2.5 \times 10^4$, $\sqrt{F} \geq 5200$ TeV ($\sqrt{F} \geq 2600$ TeV) for $N_m = 1$ ($N_m = 4$).^c In direct-transmission models, the two-loop communication between the hidden and messenger sectors is eliminated, f in Eq. (13) is effectively of order unity, and \sqrt{F} can be as low as 100 TeV in phenomenologically viable models.

Eq. (12) implies that the gravitino can be quite light for moderate \sqrt{F} values ≥ 100 TeV. For \sqrt{F} values such that $m_{\tilde{g}_{3/2}}$ is smaller than $m_{\tilde{\chi}_1^0}, m_{\tilde{\ell}_R}$, the $\tilde{g}_{3/2}$ will be the LSP. An upper bound on \sqrt{F} then arises in R-parity conserving GMSB models from the fact that the gravitino LSP is stable, and thus is also a candidate for dark matter. While very light gravitinos (eV masses) will not contribute significantly to the total mass density of the universe, if the gravitino LSP is too heavy ($m_{\tilde{g}_{3/2}} \gtrsim \text{few keV}$) its relic mass density in most early universe scenarios will be greater than the critical density [17,15] in conflict with observation.^d

From Eq. (12), this means that \sqrt{F} values above ~ 3000 TeV are disfavored. As previously noted, the helicity $\pm \frac{1}{2}$ components of $\tilde{g}_{3/2}$ behave approximately like the goldstino. In contrast to SUGRA models, F^{-1} is

^cOne should allow for a factor of two or three uncertainty in the approximate lower bound.

^dAlthough the LSP is an ideal candidate for being a major component of the dark matter, one need not use this as a constraint to restrict \sqrt{F} . It may turn out that the main component of the dark matter has another source. Some examples are: the QCD axion, its supersymmetric partner (the axino) or the lightest stable particle in the GMSB messenger sector.

now significantly larger, so that the goldstino coupling to the particles of the MSSM [Eq. (1)] is significantly enhanced relative to its SUGRA-model coupling strength. Thus, in GMSB models, the gravitino is very likely to be the LSP and will play a phenomenologically crucial role.

However, minimal GMSB is not a fully realized model. The sector of supersymmetry-breaking dynamics can be very complex, and it is fair to say that no complete model of gauge-mediated supersymmetry yet exists that is both simple and compelling. In particular, the various direct transmission models are very different from one another and from the simple hidden-sector model. Relations between sparticle and gravitino masses vary tremendously. As an extreme example, in the model of Ref. [18] the gluino is the LSP and the gravitino is sufficiently heavy as to be phenomenologically irrelevant.

4 Constraints on the gluino-LSP possibility

We have seen that it is possible in both SUGRA and GMSB models that the lightest R-hadron containing the (massive) gluino is the LSP. Thus, this rather unusual possibility deserves serious consideration.

First, there are many limits on heavy stable charged particles based on mass spectrometer searches for heavy isotopes of hydrogen and oxygen and accelerator fixed target searches for heavy new charged particles. Thus, we assume that it is the neutral $R_0 = \tilde{g}g$ that is the LSP. We assume that other neutral states such as the $\tilde{\rho}^0 = \tilde{g}(u\bar{u} + d\bar{d})$ and charged states such as the $\tilde{\rho}^+ = \tilde{g}u\bar{d}$ (and baryonic equivalents) have short lifetimes for decay to the R^0 .

Limits on a strongly interacting neutral LSP have been considered in Refs. [19,20,18]. There are many differences in these three treatments. The assessment of constraints is a very messy subject and is in a state of flux. Nonetheless, the topic is sufficiently interesting to warrant a brief overview.

As a first ingredient, we need an estimate for the relic density of R^0 's. Ref. [20], using standard freeze-out arguments and $\sigma_{\text{ann}} \sim \alpha_s^2/m_{R^0}^2$, finds $\frac{n_{R^0}}{n_B} \sim 10^{-3}m_{R^0}(\text{TeV})$, whereas Ref. [18] obtains $\frac{n_{R^0}}{n_B} \sim 10^{-7}m_{R^0}(\text{TeV})$. A factor of 10^3 in this difference appears to be due to the much larger annihilation cross section [$\sigma_{\text{ann}} \sim 40 \text{ mb} \times (m_{\text{proton}}/m_{R^0})^2$] implicitly assumed in Ref. [18]. Even for the larger relic density of Ref. [20], one finds $\frac{\rho_{R^0}}{\rho_B} \equiv \frac{n_{R^0}m_{R^0}}{n_B m_B} \sim \left(\frac{m_{R^0}}{1 \text{ TeV}}\right)^2$, implying that the R^0 cannot be the source of dark matter if $m_{R^0} \lesssim 1 \text{ TeV}$. This result, in turn, implies that if $m_{R^0} \lesssim 1 \text{ TeV}$ then it is unlikely that the galactic halo is entirely made of R^0 's.

Given a density of R^0 's, an important ingredient in obtaining limits is the flux in the vicinity of the earth of the R^0 's. If the halo density ($\rho = 0.4 \text{ GeV/cm}^3$) is dominated by R^0 's, implying $n_{R^0} = \rho/m_{R^0}$, and using

the velocity of movement of the earth through the halo ($v_{R^0} \sim 2 - 3 \times 10^7$ cm/s), the flux of R^0 's from the galactic halo would be $\phi_{R^0} = n_{R^0} v_{R^0} \sim 10^4 \left(\frac{1 \text{ TeV}}{m_{R^0}} \right) \text{ cm}^{-2} \text{ s}^{-1}$. On the other hand, if we employ the relic density $\frac{n_{R^0}}{n_B} \sim 10^{-3} m_{R^0} (\text{TeV})$ from Ref. [20] with $n_B \sim 2 \times 10^{-7} \text{ cm}^{-3}$, one finds (using the same v_{R^0}) $\phi_{R^0} \sim 6 \times 10^{-3} \left(\frac{m_{R^0}}{1 \text{ TeV}} \right) \text{ cm}^{-2} \text{ s}^{-1}$, *i.e.* much smaller for $m_{R^0} \lesssim 1 \text{ TeV}$.

Other important ingredients in obtaining limits on the R^0 are the R^0 cross sections. Ref. [20] estimates $\sigma(R^0 p) \sim 10 \text{ mb}$ and $\sigma^{\text{ann}}(R^0 R^0) \sim \alpha_s^2 / m_{R^0}^2$ (a larger value applying if the kinetic energies of the R^0 's are below a GeV or so). Ref. [18] suggests that the leading contribution to $\sigma(R^0 p)$ would come from glueball exchange: $\sigma(R^0 p) \sim 40(m_\pi / m_{\text{glueball}})^2 \text{ mb}$. Since the lightest glueball is ~ 10 times heavier than a pion, $\sigma(R^0 p)$ would then be $\lesssim 0.4 \text{ mb}$.

Limits on the R^0 derive from: (1) dark-matter (wimp) balloon and underground mine detection experiments; (2) capture and co-annihilation in the earth [19] (to produce ν 's detected in proton decay detectors, at least as secondary products of primary annihilation) or capture and co-annihilation in the halo [20] to produce energetic γ 's that are detected; (3) limits on heavy isotopes created by the flux of R^0 's impacting the earth. We consider each in turn.

(1) Ref. [20] considers only underground wimp detectors. First, they argue that since the R^0 -nuclear cross section is $\gtrsim 10^{10}$ times larger than the generic heavy neutrino cross section, the wimp detectors would certainly have detected any R^0 flux, even if only at their predicted 'relic' flux level, *if the flux makes it to the detector*. Then, the critical ingredient is the penetration depth l_p of the R^0 ; l_p tends to be large because of a small energy transfer per collision. Using a geometric estimate of $\sigma(R^0 A) \sim \pi A^{2/3} (\text{Fermi})^3$, Ref. [20] estimates $l_p \sim 50 \text{ m} \times (m_{R^0} / 1 \text{ TeV})$. The result is that for $m_{R^0} \lesssim 100 \text{ GeV}$, l_p is too small for the flux to penetrate to any wimp detectors. Of course, l_p would be further increased if the smaller $\sigma(R^0 A)$ estimate of [18] were correct. On the other hand, the applicability of these limits is more marginal if the relic flux is as small as that obtained in Ref. [18]. Further, it is important to note that the effects of energy degradation are estimated to be small in Ref. [20], whereas they are found to be sufficiently substantial in Ref. [19] as to reduce rates below observable levels in all the cases considered there (assuming the fluxes are rescaled to the relic density level).

(2) The capture and co-annihilation event rates depend upon the annihilation cross section and the fraction of the annihilation product energy appearing in the relevant channel, as well as whether or not the relevant density is halo or relic. For both types of observation, the conclusion seems to be that events

would be likely to have been seen if the density is halo-like, but probably not if relic-like.

(3) Since the R^0 can almost certainly be captured by oxygen ^e limits on exotic oxygen isotopes contained in water molecules in the ocean will place limits on the R^0 . The limits on such heavy water given in Ref. [20] require $\phi_{R^0} \lesssim 0.1 m_{R^0} (\text{TeV}) \left(\frac{100 \text{ Myr}}{t_{\text{acc}}} \right) \text{cm}^{-2} \text{s}^{-1}$, where t_{acc} is the accumulation time, with 100 Myr being an estimate for the age of the ocean. This flux limit can be compared with the fluxes computed earlier. One observes that if R^0 's are the dominant halo component, then we would require $m_{R^0} > 100 \text{ TeV}$. However, we have already argued that the halo density should not be dominated by R^0 's. The R^0 flux estimated using the Ref. [20] relic R^0 density prediction is well below the above limit. In Ref. [18] the estimated relic R^0 density is even smaller, and the dominant source of R^0 's impinging on the ocean is R^0 production in the atmosphere by cosmic rays. The crude estimate of the heavy isotope abundance arising from this source borders on the observed limit.

In summary, it appears that we can escape the above limits for $m_{R^0} \lesssim 1 \text{ TeV}$ so long as the halo density of R^0 's is similar to the (very small) relic density estimated in Ref. [18]. Alternatively, a relic density as large as that estimated in Ref. [20] is allowed if energy degradation effects are much larger than allowed for in their wimp detection estimates or if $m_{R^0} \lesssim 100 \text{ GeV}$. In either case, the R^0 's cannot be a significant source of dark matter.

5 Beyond the MSSM

Non-minimal models of low-energy supersymmetry can also be constructed. One approach is to add new structure beyond the Standard Model at the TeV scale or below. The supersymmetric extension of such a theory would be a non-minimal extension of the MSSM. Possible new structures include: (i) the supersymmetric generalization of the see-saw model of neutrino masses; (ii) an enlarged electroweak gauge group beyond $\text{SU}(2) \times \text{U}(1)$; (iii) the addition of new, possibly exotic, matter multiplets [*e.g.*, a vector-like color triplet with electric charge $\frac{1}{3}e$; such states sometimes occur as low-energy remnants in E_6 grand unification models]; (iv) the addition of low-energy $\text{SU}(3) \times \text{SU}(2) \times \text{U}(1)$ singlets; and/or (v) the addition of one or more new families with massive neutrinos.

A second approach is to retain the minimal particle content of the MSSM but remove the assumption of R-parity invariance [21]. The most general

^eWe presume that the capture rate by protons is much smaller, if not zero. Otherwise, the much stronger limits on heavy hydrogen isotopes almost certainly rule out the R^0 LSP.

explicit ^f R-parity-violating (RPV) theory involving the MSSM spectrum introduces many new parameters to both the supersymmetry-conserving and the supersymmetry-breaking sectors. Each new interaction term violates either B or L conservation. For example, new scalar-fermion Yukawa couplings would be:

$$(\lambda_L)_{pmn} \hat{L}_p \hat{L}_m \hat{E}_n^c + (\lambda'_L)_{pmn} \hat{L}_p \hat{Q}_m \hat{D}_n^c + (\lambda_B)_{pmn} \hat{U}_p^c \hat{D}_m^c \hat{D}_n^c, \quad (14)$$

where p , m , and n are generation indices, and gauge group indices are suppressed. In the notation above, \hat{Q} , \hat{U}^c , \hat{D}^c , \hat{L} , and \hat{E}^c respectively represent $(u, d)_L$, u_L^c , d_L^c , $(\nu, e^-)_L$, and e_L^c and the corresponding superpartners. The Yukawa interactions are obtained from Eq. (14) by taking all possible combinations involving two fermions and one scalar superpartner. Note that the term in Eq. (14) proportional to λ_B violates B, while the other two terms violate L.

Additional R-parity violating effects arise from the mixing of \hat{L}_p and the $Y = -1$ Higgs superfield \hat{H}_d . This leads to new parameters μ'_p ($p = 1, 2, 3$) which are analogues of the supersymmetric Higgs mass parameter μ . Finally, there are soft-supersymmetry-breaking R-parity-violating A -terms and a B -term contributing to the scalar potential (*i.e.*, the interaction of squarks, sleptons and Higgs bosons):

$$(a_L)_{pmn} \tilde{L}_p \tilde{L}_m \tilde{E}_n^c + (a'_L)_{pmn} \tilde{L}_p \tilde{Q}_m \tilde{D}_n^c + (a_B)_{pmn} \tilde{U}_p^c \tilde{D}_m^c \tilde{D}_n^c + b'_p \tilde{L}_p H_u, \quad (15)$$

where H_u is the $Y = 1$ doublet of Higgs scalars.

Phenomenological constraints on various low-energy L and B-violating processes yield limits on each of the coefficients $(\lambda_L)_{pmn}$, $(\lambda'_L)_{pmn}$ and $(\lambda_B)_{pmn}$ taken one at a time [21]. If more than one coefficient is simultaneously non-zero, then the limits are in general more complicated. All possible RPV terms cannot be simultaneously present and unsuppressed; otherwise the proton decay rate would be many orders of magnitude larger than the present experimental bound. One way to avoid proton decay is to impose B or L-invariance (either one alone would suffice). For example, models of “baryon-parity” possess a discrete symmetry that requires $\lambda_B = 0$ but allows non-zero L-violating terms in Eq. (14).

6 The Higgs sector of low-energy supersymmetric models

In the MSSM, the Higgs sector is a two-Higgs-doublet model with Higgs self-interactions constrained by supersymmetry [22,23]. After absorbing unphysical phases into the definition of the Higgs fields one finds that the Higgs sector

^fThe phenomenology of models in which there is spontaneous R-parity violation from a sneutrino field vacuum expectation value is described elsewhere in these proceedings.

is CP-conserving, so that $\tan\beta$ is a real parameter (conventionally chosen to be positive). The physical neutral Higgs scalars are CP-eigenstates. The five physical Higgs particles are those listed earlier. At tree level, $\tan\beta$ and one Higgs mass (usually chosen to be m_{A^0}) determine the tree-level Higgs-sector parameters. These include the other Higgs masses, an angle α [which measures the component of the original $Y = \pm 1$ Higgs doublet states in the physical CP-even neutral scalars], the Higgs boson self-couplings, and the Higgs boson couplings to particles of the Standard Model and their superpartners.

When one-loop radiative corrections are incorporated, the Higgs masses and couplings depend on additional parameters of the supersymmetric model that enter via virtual loops. The impact of these corrections can be significant. Most importantly, the tree-level MSSM-124 upper bound of $m_{h^0} \leq m_Z |\cos 2\beta| \leq m_Z$ is increased to $m_{h^0} \lesssim 125 - 130$ GeV for $m_t = 175$ GeV and a top-squark mass of $m_{\tilde{t}} \lesssim 1$ TeV. The charged Higgs mass is also constrained in the MSSM. At tree level, $m_{H^\pm}^2 = m_W^2 + m_{A^0}^2$, which implies that charged Higgs bosons cannot be pair produced at LEP-2. Radiative corrections modify the tree-level prediction, but the corrections are typically small.

In the parameter regime of $m_{A^0} \gtrsim 2m_Z$, one finds that the couplings of the h^0 are nearly indistinguishable from those of the Standard Model Higgs boson. Moreover, the non-minimal Higgs states, H^0 , A^0 , and H^\pm are heavy and approximately degenerate in mass. This regime, called the *decoupling limit*, is rather generic and applies also to models with more general Higgs sectors. Present experimental bounds do not yet require the Higgs sector parameters to lie in the decoupling regime. In this regard, one of the most sensitive observables is the decay rate for $b \rightarrow s\gamma$. Current data yields a rate that is within 2σ of the Standard Model prediction. Applying these results to the MSSM, the observed rate (which is *below* the Standard Model prediction) would require a negative one-loop contribution of a light chargino and top-squark to cancel the positive loop contributions of the W^\pm and H^\pm . In the absence of light supersymmetric particle loops, one obtains a strong lower bound on the charged Higgs mass, since the latter contribution raises the predicted rate for $b \rightarrow s\gamma$. In this case, one finds that $m_{A^0} \gtrsim 350$ GeV, a result well into the decoupling regime.

The MSSM Higgs mass bound quoted above does not in general apply to non-minimal supersymmetric extensions of the Standard Model. If additional Higgs singlet and/or triplet fields are introduced, then new Higgs self-coupling parameters appear, which are not significantly constrained by present data. These parameters can contribute to the light Higgs masses; the upper bound on these contributions depends on an extra assumption beyond the physics of the TeV-scale effective theory. For example, in the simplest non-minimal

supersymmetric extension of the Standard Model (NMSSM), the addition of a Higgs singlet adds a new Higgs self-coupling parameter, λ [24]. The mass of the lightest neutral Higgs boson can be raised arbitrarily by increasing the value of λ . Under the assumption that all couplings stay perturbative up to the Planck scale, one finds in almost all cases that $m_{h^0} \lesssim 150$ GeV, independent of the details of the low-energy supersymmetric model [25]. The NMSSM also permits a tree-level charged Higgs mass below m_W . However, as in the MSSM, the charged Higgs boson becomes heavy and approximately degenerate in mass with A^0 in the decoupling limit (where $m_{A^0} \gg m_Z$).

Finally, in models of R-parity violating supersymmetry, the distinction between the Higgs and matter multiplets is lost. Thus, R-parity violation permits the mixing of sleptons and Higgs bosons. The associated phenomenology will not be addressed here; see Ref. [26] for further discussion.

6.1 Supersymmetric Higgs searches at future colliders

We now consider the opportunities for detecting the Higgs bosons of R-parity conserving low-energy supersymmetry at future colliders. Over (nearly) the complete range MSSM Higgs sector parameter space, at least one of the MSSM Higgs bosons will be detectable at the LHC (if not at LEP-2 or the Tevatron), assuming that the machine runs at its design luminosity of 100 pb^{-1} per year, and under the assumption that the current detector design capabilities are achieved. An e^+e^- collider (denoted eC) or a $\mu^+\mu^-$ collider (denoted μC) would also guarantee detection of at least one Higgs boson for all of the MSSM Higgs sector parameter space (by extending the LEP-2 Higgs search) once the center-of-mass energy of the machine is above 300 GeV.

However, complete coverage of the MSSM parameter space only means that at least one Higgs boson can be detected. For example, in the decoupling limit (where $m_{A^0} \gtrsim 2m_Z$), h^0 will surely be discovered at LEP-2 or the LHC (and can be observed at the eC). But, detection of the heavier non-minimal Higgs states H^0 , A^0 , and/or H^\pm is not guaranteed. At the LHC, there is a region [27], illustrated in Fig. 3, in the $(m_{A^0}, \tan\beta)$ parameter space characterized by $\tan\beta \gtrsim 3$ and $m_{A^0} \gtrsim 300$ GeV ^g such that only the h^0 will be detectable. ^h At the eC , H^0A^0 and H^+H^- pair production is not kinematically allowed if $m_{A^0} \gtrsim \sqrt{s}/2$. Moreover, the production rate for h^0A^0 (although it may

^gThis is probably the only region of Fig. 3 that is consistent with the measured $BF(b \rightarrow s\gamma)$ given that $m_{\tilde{t}} \sim 1$ TeV is assumed.

^h In the regime $1 \lesssim \tan\beta \lesssim 3$ and $m_{A^0} \gtrsim 300$ GeV, Ref. [27] asserts that A^0 and H^0 can be discovered at the LHC via their $t\bar{t}$ decay mode. However, there has not been a full detector simulation and complete analysis of backgrounds to substantiate such a claim.

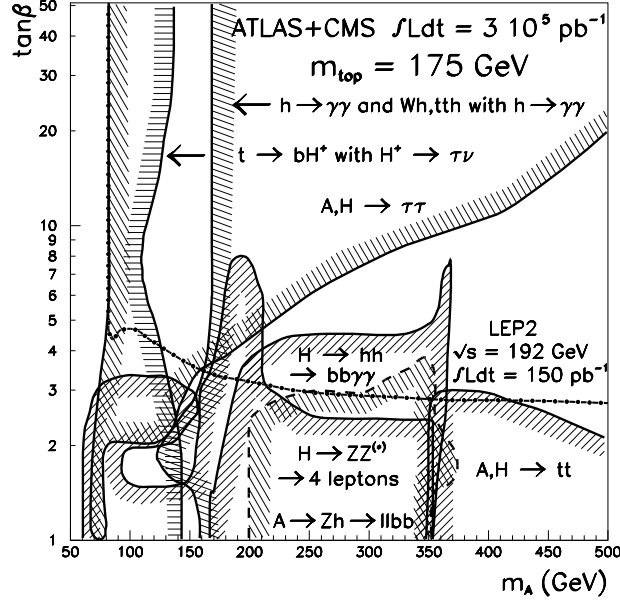


Figure 3: Discovery contours (5σ) in the parameter space of the minimal supersymmetric model for ATLAS+CMS at the LHC: $L = 300 \text{ fb}^{-1}$. Two-loop/RGE-improved radiative corrections to the MSSM Higgs sector are included assuming $m_{\tilde{t}} = 1 \text{ TeV}$ and no squark mixing.

be kinematically allowed) is suppressed in the decoupling limit. Thus, the non-minimal Higgs states are not detectable at the eC for $m_{A^0} \gtrsim \sqrt{s}/2$.

Recently, two important questions regarding the observation of the Higgs sector of a supersymmetric model have been addressed.

- First, is discovery of one Higgs boson guaranteed if singlet Higgs fields are added to the MSSM?

1. It has been demonstrated [28] that at least one of the light CP-even Higgs bosons ($h_{1,2,3}$) of a two-doublet plus one singlet NMSSM Higgs sector will be observed at the eC . This result follows from the fact that if the lightest (h_1) has weak ZZ coupling then (one of) the heavier ones must be almost as light and have substantial ZZ coupling (and thus be discoverable in the $e^+e^- \rightarrow Z^* \rightarrow Zh$ production mode). This result probably extends to models

that contain several singlet Higgs fields.

2. However, before the eC is built, only data from LEP-2, the Tevatron and the LHC will be available. One finds [29] that discovery of at least one Higgs boson is no longer guaranteed if a singlet Higgs field is present in addition to the minimal two doublet fields. The no-discovery “holes” in parameter space are never terribly large, but are certainly not insignificant for moderate values of $\tan\beta \sim 3$ –10.

In order to demonstrate point 2. above, one employs the same detection modes for the NMSSM as employed for Fig. 3 in the MSSM case: (1) $Z^* \rightarrow Zh$ at LEP-2; (2) $Z^* \rightarrow ha$ at LEP-2; (3) $gg \rightarrow h \rightarrow \gamma\gamma$ at the LHC; (4) $gg \rightarrow h \rightarrow ZZ^*$ or $ZZ \rightarrow 4\ell$ at LHC; (5) $t \rightarrow H^+b$ at the LHC; (6) $gg \rightarrow b\bar{b}h, b\bar{b}a \rightarrow b\bar{b}\tau^+\tau^-$ at the LHC; (7) $gg \rightarrow h, a \rightarrow \tau^+\tau^-$ at the LHC. Additional Higgs decay modes that could be considered, but not reliably, at the LHC include: (a) $a \rightarrow Zh$; (b) $h \rightarrow aa$; (c) $h_j \rightarrow h_i h_i$; (d) $a, h \rightarrow t\bar{t}$. In order to avoid having to consider these latter, we explicitly exclude any choice of NMSSM parameters for which (a)-(d) might be relevant.

The free parameters specifying the Higgs sector of the NMSSM are: $\tan\beta$, the mass of the lightest CP-even Higgs mass eigenstate m_{h_1} , the mass of the lightest CP-odd scalar m_a (we consider only the parameter sub-region in which the 2nd CP-odd scalar is taken to be much heavier), the new superpotential coupling λ appearing in $W \ni \lambda \hat{H}_d \hat{H}_u \hat{N}$, and three mixing angles $\alpha_{1,2,3}$ which parameterize the orthogonal matrix that diagonalizes the CP-even Higgs mass-squared matrix. One finds that $\lambda \lesssim 0.7$ is required if λ is to remain perturbative during evolution from m_Z to M_U , which implies a $\tan\beta$ -dependent upper limit on m_{h_1} below ~ 140 GeV.

As already noted, moderate $\tan\beta$ yields the worst case: for low $\tan\beta \leq 1.5$, at least one of the CP-even Higgs is observable in the standard $\gamma\gamma, 4\ell, \dots$ modes; at high $\tan\beta \geq 10 - 11$, the $b\bar{b}h$ and $b\bar{b}a$ modes (with h, a decaying to $\tau^+\tau^-$) are sufficiently enhanced to be observable. A typical unobservable region of $(\alpha_1, \alpha_2, \alpha_3)$ parameter space that arises at moderate $\tan\beta$ is illustrated in Fig. 4.

3. At a $\mu^+\mu^-$ collider, direct s -channel production $\mu^+\mu^- \rightarrow h_1$ is quite likely to be visible [30]. Only the (predicted) $\mu^+\mu^-h_1$ coupling is needed; the h_1 can be decoupled from ZZ, WW without affecting its detectability. If the h_1 has not been previously detected, then a scan search in the $m_{h_1} \leq 150$ GeV region is required with $\Delta E_{\text{beam}}/E_{\text{beam}} \lesssim 0.01\%$. The time required for this scan could run to many years, depending upon the luminosity of the muon-collider (μC) and the size of the $\mu^+\mu^-h_1$ coupling.

- A second important question is: What is required in order to discover

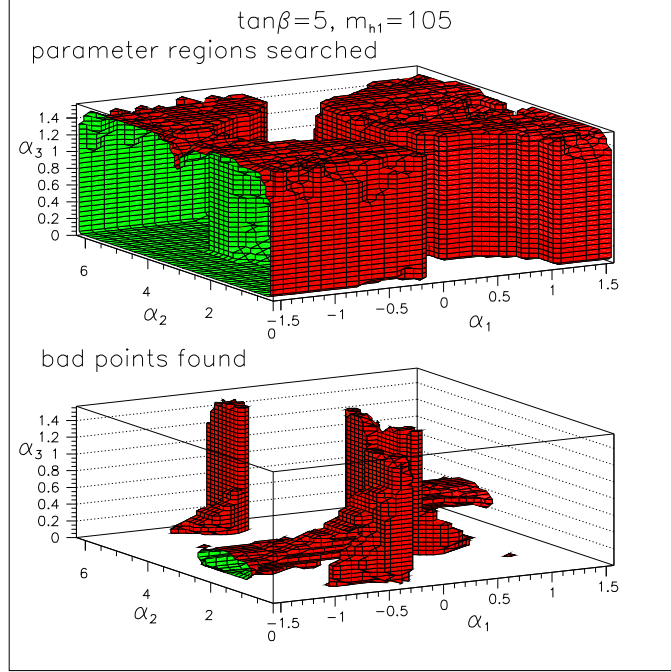


Figure 4: For $\tan \beta = 5$ and $m_{h_1} = 105$ GeV, we display in three dimensional $(\alpha_1, \alpha_2, \alpha_3)$ parameter space the parameter regions searched (which lie within the surfaces shown), and the regions therein for which the remaining model parameters can be chosen so that no Higgs boson is observable (interior to the surfaces shown).

the H^0, A^0, H^\pm of the MSSM?

Here, a region of particular concern is the decoupling regime of $m_{A^0} \gtrsim 200$ GeV, where finding evidence for a non-minimal Higgs sector will be the most problematical. This concern is most pronounced if $\tan \beta \gtrsim 3$, *i.e.* such that the LHC cannot observe the H^0, A^0 (see above).

1. At the eC , the only means for detecting any of the heavier non-minimal Higgs states H^0, A^0, H^\pm when $m_{A^0} \gtrsim \sqrt{s}/2$ is to run the collider in the $\gamma\gamma$ collider mode [31,32]. In this way, single $\gamma\gamma \rightarrow H^0, A^0$ production can be observed for $m_{A^0} \lesssim 0.8\sqrt{s}$ provided high integrated luminosity (*e.g.*, $L \sim 200 \text{ fb}^{-1}$) is accumulated. There is still no certainty that a $\gamma\gamma$ collider facility will be included in the final eC plans, nor any guarantee that the required luminosity can be achieved.

2. At a $\mu^+\mu^-$ collider, direct s -channel production $\mu^+\mu^- \rightarrow H^0, A^0$ may

be observable [33]. Assuming no constraints on or knowledge of m_{A^0} , one would ideally wish to scan the entire region of m_{A^0} between $\sqrt{s}/2$ (the pair production limit) and the maximum available \sqrt{s} and be certain of seeing the H^0, A^0 signal (if present) for any $\tan\beta \gtrsim 3$ (the value below which the LHC will find the H^0, A^0). For $\sqrt{s} \sim 500$ GeV, this would require an integrated luminosity of $L = 100 \text{ fb}^{-1}$ (at modest beam energy resolution of 0.1%). However, current μC designs suggest that only $L \lesssim 10 \text{ fb}^{-1}/\text{yr}$ will be achieved in this energy range. Thus, if we imagine devoting a period of several years to this scan, H^0, A^0 discovery at the μC would only be certain if $\tan\beta \gtrsim 5-6$. As described shortly, the situation would be greatly improved if the h^0 has been detected and its properties measured at the $e\text{C}$ (operating at $\sqrt{s} = 500$ GeV) and/or the μC (operating in the s -channel Higgs production mode). If only $e\text{C}$ data is available, it would be possible to distinguish between the h^0 and h_{SM} and at least roughly determine m_{A^0} so long as m_{A^0} is below 450 GeV. If we only have s -channel μC data the result is similar. If both types of data are available, a rough m_{A^0} determination would be possible up to $m_{A^0} \sim 600$ GeV. Precision measurements of the SM-like Higgs properties would thus allow a much narrower scan for H^0, A^0 discovery; as a result, the H^0, A^0 could be detected at the μC with only one or two years running for essentially any $\tan\beta \gtrsim 1-2$.

3. At both the e^+e^- and $\mu^+\mu^-$ colliders, it is envisioned that the machine will be upgraded to increasingly larger \sqrt{s} . Once $\sqrt{s} \gtrsim 2m_{A^0}$, $H^0 A^0$ and $H^+ H^-$ pair production will be observable. It has been shown that this will be true even if these Higgs bosons have substantial decays to supersymmetric particles [34,35].

Returning to the MSSM Higgs sector, there are a number of interesting issues.

- How precisely will we know m_{h^0} and how useful will it be?

Certainly m_{h^0} will be very precisely measured: $\Delta m_{h^0} \lesssim 100$ MeV or better is achievable at the $e\text{C}$ and LHC; the μC yields $\Delta m_{h^0} \lesssim 1$ MeV via an s -channel scan. Precise knowledge of m_{h^0} has the potential to inaugurate a new precision game. At one-loop (neglecting mixing, *etc.*), $\Delta m_{h^0}^2 = \frac{3g^2 m_t^4}{8\pi^2 m_W^2} \ln \frac{m_t^2}{m_{\tilde{t}}^2}$. For $m_{h^0} = 100$ GeV, $\Delta m_{h^0} = \pm 100$ MeV implies constraints of order $\Delta m_t = \pm 170$ MeV, $\Delta m_{\tilde{t}} = \pm 2$ GeV. (More generally and at two-loops, A and μ parameters enter.) This level of constraint on $m_{\tilde{t}}$... probably exceeds that achievable experimentally by direct measurements. However, there is an important caveat: can theoretical predictions for m_{h^0} be made at the $\Delta m_{h^0} = \pm 100$ MeV level? The currently available two-loop RGE-improved result is only reliable to a few GeV.

- What are the prospects for and means for distinguishing the MSSM h^0 or other SM-like light Higgs bosons from the SM h_{SM} via branching ratios and couplings, and what are the implications?

We can only present a very brief summary. Further details can be found in [36] and [37]. The Snowmass96 study [36] shows that LEP-2, TeV-33 and LHC data will not provide determinations of the Higgs couplings of sufficient accuracy to distinguish the h^0 from the h_{SM} in the ‘decoupling’ regime of $m_{A^0} \gtrsim 2m_Z$. For example, for a SM-like Higgs mass $\sim m_Z$ (the best case where data from all three machines will be available) the fundamental properties that can be determined (which is a limited subset) and their errors are: $BF(b\bar{b}) - \pm 26\%$; $(WWh_{SM})^2/(ZZh_{SM})^2 - \pm 14\%$; $(WWh_{SM})^2 - \pm 20\%$; $(ZZh_{SM})^2 - \pm 22\%$; $(\gamma\gamma h_{SM})^2/(b\bar{b}h_{SM})^2 - \pm 17\%$; $BF(\gamma\gamma) - \pm 31\%$; $(ggh_{SM})^2 - \pm 31\%$; $(t\bar{t}h_{SM})^2/(WWh_{SM})^2 - \pm 21\%$; $(t\bar{t}h_{SM})^2 - \pm 30\%$. At higher masses, LEP-2 data will not be available and TeV-33 statistics decline rapidly. Overall, without eC and/or μC data, we will know that the Higgs is SM-like, but we will not be able to discriminate between different SM-like possibilities.

As a next step, we imagine that we have data available from the eC as well as the LHC. This yields a dramatic improvement in our ability to determine the fundamental couplings of the h^0 . One finds [36] that the best ‘bet’ for discriminating between SM-like Higgs bosons for $m_h \leq 130$ GeV is via the ratio $\sigma BF(h \rightarrow c\bar{c})/\sigma BF(h \rightarrow b\bar{b})$; for $m_h \geq 130$ GeV (as possibly relevant in the NMSSM), $\sigma BF(h \rightarrow WW^*)/\sigma BF(h \rightarrow b\bar{b})$ will be the most valuable ratio. The results from Snowmass96 use ‘topological tagging’ (*e.g.* primary, secondary, tertiary vertices for a b jet but only primary and secondary vertices for a c jet). For $L = 200 \text{ fb}^{-1}$ at $\sqrt{s} = 500$ GeV and $m_h \leq 130$ GeV (and combining Zh , ZZ -fusion and WW -fusion production processes), one obtains a statistical error in $BF(c\bar{c})/BF(b\bar{b})$ of $\sim \pm 7\%$. Theoretical uncertainty in $m_c(m_c)$ and $m_b(m_b)$ (sum rules, lattice) and QCD running should reach the $< 10\%$ level in a few years, implying a net error of $\lesssim 10\%$. The result is that one would be able to distinguish h^0 from h_{SM} at a $\geq 2\sigma$ level for $m_{A^0} \leq 450$ GeV for the typical $m_{h^0} = m_{h_{SM}} = 110$ GeV mass case. This is illustrated in Fig. 5, where it is seen that deviations are almost independent of $\tan\beta$ and are larger than $\sim 20\%$ for $m_{A^0} \leq 450$ GeV.

For the NMSSM, the determination of the $(ZZh)^2$ coupling squared could be very valuable for checking the sum rule $\sum_i (ZZh_i)^2 = \sum_i (WWh_i)^2 = 1$, (where the $(VVh_i)^2 - V = W, Z$ – are defined relative to the SM-values).^{*i*} A direct measurement (independent of the h branching ratios) is possible using $e^+e^- \rightarrow Zh$ with $Z \rightarrow e^+e^-, \mu^+\mu^-$ and $e^+e^- \rightarrow e^+e^-h$ (ZZ -fusion) produc-

^{*i*} $(ZZh)^2$ is also crucial to getting many quantities in eC only analysis.

NLC, Zh Mode: MSSM/SM Ratio Contours

$m_{\text{TOP}}=175$ GeV, $m_h=110$ GeV, Max. Mix.

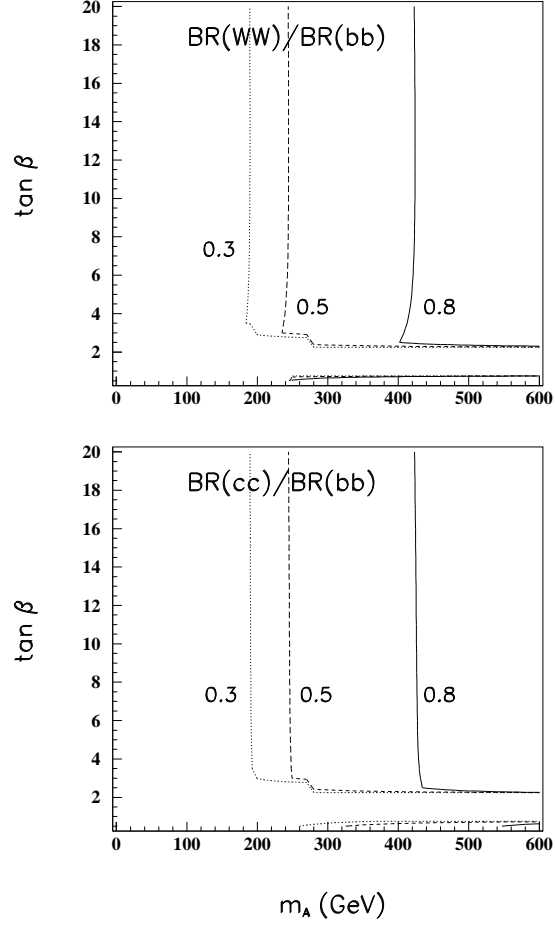


Figure 5: Constant value contours in $(m_{A^0}, \tan \beta)$ parameter space for the ratios $[WW^*/b\bar{b}]_{h^0}/[WW^*/b\bar{b}]_{h_{SM}}$ and $[c\bar{c}/b\bar{b}]_{h^0}/[c\bar{c}/b\bar{b}]_{h_{SM}}$. We assume “maximal mixing” in the squark sector and present results for the case of fixed $m_{h^0} = m_{h_{SM}} = 110$ GeV. The band extending out to large m_{A^0} at $\tan \beta \sim 2$ is where $m_{h^0} = 110$ GeV is theoretically disallowed in the case of maximal mixing. For no mixing, the vertical contours are essentially identical — only the size of the disallowed band changes. The same contours apply if $b\bar{b}$ is replaced by $\tau^+\tau^-$.

tion and isolation of the h as a peak in the missing mass recoiling against the $\ell^+\ell^-$. Inclusion of the ZZ -fusion mode [38] as well as the usual Zh associated production mode, yields $(ZZh)^2$ errors in the $m_h < 150$ GeV range of order $\pm 5\% - \pm 7\%$. Determining $(WWh)^2$ is more involved. For example, for $m_h \leq 140$ GeV, one must measure $\sigma(\nu\bar{\nu}h)BF(h \rightarrow b\bar{b})$, and divide by $BF(h \rightarrow b\bar{b})$. One can determine $BF(h \rightarrow b\bar{b})$, from the ratios of the type $\sigma(Zh)BF(h \rightarrow b\bar{b})/\sigma(Zh)$ and the ZZ fusion analogue, with an accuracy of about 5% for $m_h \lesssim 130$ GeV (assuming a SM-like h). The result is $\sim \pm 5\% - \pm 6\%$ error for $(WWh)^2$ when $m_h \leq 140$ GeV.

Determination of Γ_h^{tot} (as needed needed to compute $(Xh)^2 = BF(h \rightarrow X)\Gamma_h^{\text{tot}}$ for $X = b\bar{b}$, etc.) requires a lengthy indirect procedure for $m_h \leq 130$ GeV. One needs to determine $BF(h \rightarrow \gamma\gamma)$ as well as possible and use $\gamma\gamma$ collisions to determine $\Gamma(h \rightarrow \gamma\gamma)$ and then compute $\Gamma_h^{\text{tot}} = \frac{\Gamma(h \rightarrow \gamma\gamma)}{BF(h \rightarrow \gamma\gamma)}$. Unfortunately, $BF(h \rightarrow \gamma\gamma)$ cannot be well measured at eC alone. The best results are obtained by using a complicated procedure involving LHC and eC data, as described in Ref. [36]. The net result is an $BF(h \rightarrow \gamma\gamma)$ error of $\lesssim \pm 16\%$ for $m_h \lesssim 130$ GeV. To measure $\Gamma(h_{SM} \rightarrow \gamma\gamma)$, the $\gamma\gamma$ collider is required. Current estimates, including systematics, suggest a $\Gamma(h_{SM} \rightarrow \gamma\gamma)BF(h_{SM} \rightarrow b\bar{b})$ error (for $L = 50 \text{ fb}^{-1}$ at the $\gamma\gamma$ collider) of 8%-10%. Given $\pm 5\% - \pm 6\%$ error for $BF(h_{SM} \rightarrow b\bar{b})$ one finds a $\Gamma(h_{SM} \rightarrow \gamma\gamma)$ error of order $\pm 12\%$. Putting all this together yields a $\Gamma_{h_{SM}}^{\text{tot}}$ error of $\sim \pm 18\%$; not very wonderful. A detailed summary of errors for branching ratios, couplings and the total width of a SM-like Higgs obtained by combining LHC, eC and $\gamma\gamma$ collider data appears in Ref. [36].

Production of the h in the s -channel at a muon collider can provide even greater discrimination power between the h^0 and the h_{SM} , provided $m_h \neq m_Z$ [33]. The crucial measurements are two: (1) The very tiny Higgs width: $\Gamma_h^{\text{tot}} = 1 - 10 \text{ MeV}$ for a SM-like Higgs with $m_h \lesssim 140$ GeV (i.e. mass as predicted for the h^0 of the MSSM). (2) $\sigma(\mu^+\mu^- \rightarrow h \rightarrow X)$ for $X = \tau^+\tau^-, c\bar{c}, b\bar{b}, WW^*, ZZ^*$.^j The accuracies estimated to be achievable during an optimized 3-point scan with total integrated luminosity of $L = 0.4 \text{ fb}^{-1}$ (as currently projected for four years of operation with a beam energy resolution of $R = 0.003\%$) in the case of $m_{h^0} = 110$ GeV are the following: $\tau^+\tau^- \rightarrow \pm 8\%$; $c\bar{c} \rightarrow \pm 19\%$; $b\bar{b} \rightarrow \pm 3\%$; $WW^* \rightarrow \pm 15\%$; $ZZ^* \rightarrow \pm 190\%$; $\Gamma_{h_{SM}}^{\text{tot}} \rightarrow \pm 16\%$. The important ratios for discriminating h^0 from h_{SM} , and their errors, are: $\frac{WW^*}{\tau^+\tau^-} \rightarrow \pm 18\%$, $\frac{c\bar{c}}{\tau^+\tau^-} \rightarrow \pm 22\%$, $\frac{WW^*}{b\bar{b}} \rightarrow \pm 15\%$, $\frac{c\bar{c}}{b\bar{b}} \rightarrow \pm 20\%$. From Fig. 5, these errors imply that with $L = 0.4 \text{ fb}^{-1}$ at the μC one can distinguish

^jNote that $\sigma(\mu^+\mu^- \rightarrow h \rightarrow X)$ provides a determination of $\Gamma(h \rightarrow \mu^+\mu^-)BF(h \rightarrow X)$ unless $\sigma_{\sqrt{s}} \ll \Gamma_h^{\text{tot}}$.

between the h_{SM} and the h^0 at a $> 2\sigma$ level for m_{A^0} up to ~ 400 GeV, which is similar to the discrimination power of the eC operating at $\sqrt{s} = 500$ GeV for $L = 200 \text{ fb}^{-1}$. Note that since the Γ_h^{tot} errors are big and since Γ_h^{tot} is model-dependent, Γ_h^{tot} is not so clearly useful as the above ratios. Still, deviations of $\Gamma_{h^0}^{\text{tot}}$ from $\Gamma_{h_{SM}}^{\text{tot}}$ are predicted to be substantial if $m_{A^0} \lesssim 500$ GeV.

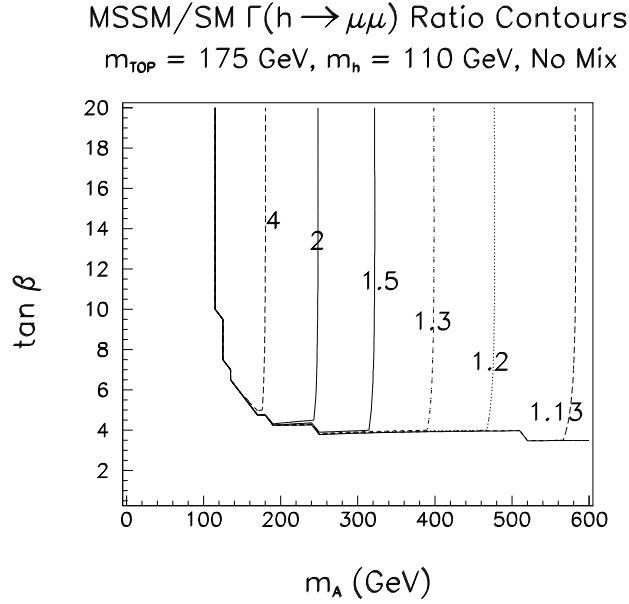


Figure 6: Constant value contours in $(m_{A^0}, \tan \beta)$ parameter space for the ratio $\Gamma(h^0 \rightarrow \mu^+\mu^-)/\Gamma(h_{SM} \rightarrow \mu^+\mu^-)$. We assume “no mixing” in the squark sector and present results for the case of fixed $m_{h^0} = m_{h_{SM}} = 110$ GeV. For “maximal mixing”, the vertical contours are essentially identical — only the size of the allowed parameter range is altered. Contours for $\Gamma(h^0 \rightarrow b\bar{b})/\Gamma(h_{SM} \rightarrow b\bar{b})$ are identical.

Finally, let us consider what can be achieved if eC (or equivalent muon-collider) $\sqrt{s} = 500$ GeV data ($L = 200 \text{ fb}^{-1}$), is combined with s -channel μC data. The most powerful discriminator between the h^0 and h_{SM} turns out to be $\Gamma(h \rightarrow \mu^+\mu^-)$. This is because there are four statistically independent ratios that can be used to determine $\Gamma(h \rightarrow \mu^+\mu^-)$:

$$(1) \quad \frac{[\Gamma(h_{SM} \rightarrow \mu^+\mu^-)BF(h_{SM} \rightarrow b\bar{b})]_{\mu C}}{BF(h_{SM} \rightarrow b\bar{b})_{eC}};$$

$$\begin{aligned}
(2) \quad & \frac{[\Gamma(h_{SM} \rightarrow \mu^+ \mu^-) BF(h_{SM} \rightarrow WW^*)]_{\mu C}}{BF(h_{SM} \rightarrow WW^*)_{eC}}; \\
(3) \quad & \frac{[\Gamma(h_{SM} \rightarrow \mu^+ \mu^-) BF(h_{SM} \rightarrow ZZ^*)]_{\mu C} [\Gamma_{h_{SM}}^{\text{tot}}]_{eC+\mu C}}{\Gamma(h_{SM} \rightarrow ZZ^*)_{eC}}; \\
(4) \quad & \frac{[\Gamma(h_{SM} \rightarrow \mu^+ \mu^-) BF(h_{SM} \rightarrow WW^*) \Gamma_{h_{SM}}^{\text{tot}}]_{\mu C}}{\Gamma(h_{SM} \rightarrow WW^*)_{eC}}.
\end{aligned}$$

At $m_h = 110$ GeV, the error for $\Gamma(h \rightarrow \mu^+ \mu^-)$ that results from combining all these determinations is $\sim \pm 4\%$. (This error only increases to $\sim \pm 5\%$ if the μC s -channel integrated luminosity is decreased from 0.4 fb^{-1} to 0.1 fb^{-1} , for example.) Given that there is no systematic uncertainty in the prediction for $\Gamma(h \rightarrow \mu^+ \mu^-)$ (m_μ is precisely known), we see from Fig. 6 that $\Gamma(h \rightarrow \mu^+ \mu^-)$ provides a 3σ level of discrimination between the h_{SM} and the h^0 all the way out to $m_{A^0} \gtrsim 600$ GeV. Similar results apply so long a m_h is not in the vicinity of m_Z .

The importance of determining the SM-like Higgs properties with the greatest possible precision argues strongly for having *both* a eC and a μC , especially since very substantial accumulated luminosity is needed at *both* machines in order to achieve good precision for a model-independent determination of all the Higgs couplings and its total width.

- What can we learn from the branching ratios of the H^0, A^0 in the supersymmetric GUT context?

Once the H^0, A^0 and/or H^\pm have been detected (either in s -channel production at a μC or in pair production at the eC), it will be possible to measure their branching ratios to various final states with substantial precision. Refs. [34,35] have demonstrated that such measurements, in combination with a determination of m_{A^0} and one of the gaugino masses, will allow determination of a large number of the MSSM parameters, thereby discriminating between different sets of initial M_U boundary conditions. In particular, Ref. [34] shows that expected accuracies for supersymmetric mode decays in pair production will allow one to discriminate at a very high confidence level between different boundary condition models. Thus, Higgs pair production will be a powerful tool in determining the correct GUT-scale boundary conditions.

Additional issues/questions that we do not have room to address in detail relate to a Higgs sector with CP-violation. If the Higgs sector is found to be CP-violating, then the MSSM is ruled out. However, the NMSSM and its extensions can have CP violation in the Higgs sector. Recent work in this area includes:

- The development of a new sum rule for Higgs couplings and its use to extract limits from LEP-2 for a CP-violating general (non-MSSM) two Higgs doublet model (2HDM) or two-doublet plus one singlet (2D1S) Higgs sector [39]. The sum rule can be used to show that LEP-2 data excludes the possibility that there can be two light Higgs bosons in the CP-violating 2HDM or three light Higgs bosons in the 2D1S model.
- Development of optimal procedures for precision measurement of the couplings, including CP-violating couplings, for a neutral Higgs boson at a high energy e^+e^- collider by combining $t\bar{t}h$ and Zh production data [40]. One finds that truly excellent errors/limits on all couplings should be attainable. Prospects for determining the CP properties of a Higgs boson at the LHC using $t\bar{t}h$ associated production are also not insubstantial [41].

7 The lightest and next-to-lightest supersymmetric particles

The phenomenology of low-energy supersymmetry depends crucially on the properties of the lightest supersymmetric particle (LSP). In R-parity conserving low-energy supersymmetry, all Standard Model particles are R-even while their superpartners are R-odd. Thus, starting from an initial state involving ordinary (R-even) particles, it follows that supersymmetric particles must be produced in pairs. In general, these particles are highly unstable and decay quickly into lighter states. However, R-parity invariance also implies that the LSP is absolutely stable, and must eventually be produced at the end of a decay chain initiated by the decay of a heavy unstable supersymmetric particle.

In order to be consistent with cosmological constraints, a stable LSP is almost certainly electrically and color neutral. Consequently (with the exception of a gluino-LSP), the LSP in an R-parity-conserving theory is weakly-interacting in ordinary matter, *i.e.* it behaves like a stable heavy neutrino and will escape detectors without being directly observed. Thus, the canonical signature for conventional R-parity-conserving supersymmetric theories is missing (transverse) energy, due to the escape of the LSP.

As noted earlier, in mSUGRA models the LSP is likely to be the $\tilde{\chi}_1^0$ (as opposed to the gravitino) and it tends to be dominated by its U(1)-gaugino component (but, see below). A nearly pure U(1)-gaugino (sometimes called a *bino*) will be denoted by \tilde{B} . However, there are some regions of mSUGRA parameter space where other possibilities for the LSP are realized. For example, there are regions of mSUGRA parameter space where the LSP is a chargino. These regions must be excluded since we reject the possibility of charged relic particles surviving the early universe. A sneutrino LSP is possible in mSUGRA

models only if $m_{\tilde{\nu}} \lesssim 80$ GeV. In addition, the requirement that relic LSP's do not “overclose” the universe by contributing a mass density that is larger than the critical density of the universe rules out additional regions of mSUGRA parameter space. Requiring that the relic density of LSP's constitutes a significant part of the dark matter would impose further restrictions on the mSUGRA parameter space.

In more general SUGRA models, the nature of the LSP need not be so constrained. One can envision a $\tilde{\chi}_1^0$ -LSP which has an arbitrary mixture of gaugino and higgsino components by relaxing gaugino mass unification. A nearly pure wino LSP (denoted \tilde{W}) is the result if $M_2 < M_1$. A nearly pure higgsino LSP (denoted by \tilde{H}) is possible in the region where the gaugino Majorana masses satisfy $M_1 \simeq M_2 \gtrsim \mu$. The sneutrino can be a viable LSP (with no mass restriction as in mSUGRA models), although it is unlikely to be a major component of the dark matter. Finally, as described earlier, the gluino (more strictly speaking an R-hadron containing the gluino, *e.g.* $R^0 = \tilde{g}g$) can be the LSP [6].

In simple GMSB models, it was noted earlier that the mass of the gravitino lies in the eV–keV regime. Thus, in such models, the gravitino is the LSP, and the next-to-lightest supersymmetric particle (NLSP) also plays a crucial role in the phenomenology of supersymmetric particle production and decay. Note that unlike the LSP, the NLSP can be charged. In GMSB models, the most likely candidates for the NLSP are $\tilde{\chi}_1^0$ and $\tilde{\tau}_R^\pm$.^k The NLSP will decay into its superpartner plus a gravitino [either $\tilde{\chi}_1^0 \rightarrow N\tilde{g}_{3/2}$ ($N = \gamma, Z$, or h^0) or $\tilde{\tau}_R^\pm \rightarrow \tau^\pm\tilde{g}_{3/2}$], with a lifetime that is quite sensitive to the model parameters. In a small range of parameter space, it is possible that several of the next-to-lightest supersymmetric particles are sufficiently degenerate in mass such that each one behaves as the NLSP. In this case, these particles will be called co-NLSP's [42].

Different choices for the identity of the NLSP and its decay rate lead to a variety of distinctive supersymmetric phenomenologies [43,44,45,46,47,48,49]. These will be examined in detail later.

A possible exception to the above gravitino LSP scenario is that discussed earlier. It is possible [18] to construct a GMSB model in which the gluino is the LSP and the gravitino is much heavier (and, thus, phenomenologically

^kIn GMSB models, the $\tilde{\tau}_R$ tends to be the lightest slepton. It is lighter than \tilde{e}_R and $\tilde{\mu}_R$ because of the effect of the larger τ -lepton-Higgs Yukawa coupling on the evolution of scalar masses from the messenger scale to the electroweak scale. Note that the same Yukawa coupling is responsible for $\tilde{\tau}_R$ - $\tilde{\tau}_L$ mixing, so that the light $\tilde{\tau}$ mass eigenstate would not be a pure $\tilde{\tau}_R$. Nevertheless, the $\tilde{\tau}_R$ component of the lighter $\tilde{\tau}$ would dominate, so we ignore this distinction in the notation.

irrelevant). The resulting phenomenology (to be discussed later) is not dissimilar to that associated with the SUGRA gluino-LSP case mentioned earlier in association with the O-II model studied in [6].

Finally, we re-emphasize that restrictions on the SUGRA and GMSB model parameter spaces can arise from requiring that the relic LSP density not overclose the universe, but that it is premature to consider parameter restrictions based upon requiring that the LSP be the primary component of dark matter; there are other possible sources of dark matter in all models.

8 Classes of supersymmetric signals

Due to a lack of knowledge of the origin and structure of the supersymmetry-breaking parameters, the predictions of low-energy supersymmetry depend on a plethora of unknown parameters. Many details of supersymmetric phenomenology are strongly dependent on the underlying assumptions of the model. Nevertheless, we can broadly classify supersymmetric signals at future colliders by considering the various theoretical approaches described earlier. In this section, we examine a variety of supersymmetric signatures, and in the next section we explore their consequences for experimentation at future colliders.

8.1 Missing energy signatures

In R-parity conserving low-energy supersymmetry, supersymmetric particles are produced in pairs. The subsequent decay of a heavy supersymmetric particle generally proceeds via a multi-step decay chain [50], ending in the production of at least one supersymmetric particle which is weakly interacting and escapes the collider detector. Thus, supersymmetric particle production yields events that contain at least two escaping non-interacting particles, leading to a missing energy signature.^{*l*} (Only the missing transverse energy \cancel{E}_T can be determined at hadron colliders.)

In conventional SUGRA-based models, all supersymmetric events contain at least two LSP's which will escape the collider detector. This leads to the “smoking-gun” signature of low-energy supersymmetry: events with large missing transverse energy in association with jets and/or leptons. However, there

^{*l*}We are aware of only two counterexamples. First, there are models in which the $\tilde{\chi}_1^0$ is the LSP and the lightest neutralino and chargino are nearly degenerate in mass. If the mass difference is $\lesssim 100$ MeV, then $\tilde{\chi}_1^\pm$ is long-lived and decays outside the detector [51,6]. Second, there is the gluino-LSP scenario [6,18], the signatures for which will be elaborated upon later.

are two unconventional approaches in which the smoking-gun signature is absent. First, there is the model in which the $\tilde{\chi}_1^0$ is the LSP but the lightest neutralino and chargino are nearly degenerate in mass. If the mass difference is $\lesssim 100$ MeV, then the $\tilde{\chi}_1^0$ is long-lived and decays outside the detector [51,6]. Second, there is the gluino-LSP scenario. Since a hadronic calorimeter measures only the gluino kinetic energy, events in which the gluino (more precisely, the lightest R-hadron) is absorbed in or passes through the hadronic calorimeter would also have substantial missing energy; see later discussion. However, there would be no jets arising from \tilde{g} decays in such models.

In conventional GMSB models, all supersymmetric events contain at least two NLSP's, and the resulting signature depends on the NLSP properties. Four physically distinct possible scenarios emerge:

- (1) The NLSP is electrically and color neutral and long-lived, and decays outside of the detector to its associated Standard Model partner and the gravitino.
- (2) The NLSP is the sneutrino and decays invisibly into $\nu\tilde{g}_{3/2}$ either inside or outside the detector.

In either of these two cases, the resulting missing-energy signal is then similar to that of the SUGRA-based models where $\tilde{\chi}_1^0$ or $\tilde{\nu}$ is the LSP.

- (3) The NLSP is the $\tilde{\chi}_1^0$ and decays inside the detector to $N\tilde{g}_{3/2}$, where $N = \gamma, Z$ or a neutral Higgs boson.

In this case, the gravitino-LSP behaves like the neutralino or sneutrino LSP of the SUGRA models. But, the missing energy events in this case are characterized by the associated production of (at least) two N 's, one for each LSP.^m Note that if $\tilde{\chi}_1^0$ is lighter than the Z (and h^0) then $\text{BR}(\tilde{\chi}_1^0 \rightarrow \gamma\tilde{g}_{3/2}) = 100\%$, and all supersymmetric production will result in missing energy events with at least two associated photons.

- (4) The NLSP is a charged slepton (typically $\tilde{\tau}_R$ in GMSB models if $m_{\tilde{\tau}_R} < m_{\tilde{\chi}_1^0}$), which decays to the corresponding lepton partner and gravitino.

If the decay is prompt, then one finds missing energy events with associated leptons (taus). If the decay is not prompt, one observes a long-lived heavy semi-stable charged particle with *no* associated missing energy (prior to the decay of the NLSP).

^mIf the decay of the NLSP is not prompt, it is possible to produce events in which one NLSP decays inside the detector and one NLSP decays outside of the detector.

As noted earlier, there are GMSB scenarios in which there are several next-to-lightest supersymmetric particles (co-NLSP's) that are almost degenerate, in particular sufficiently degenerate that decays down to the true NLSP have a very long lifetime. The canonical example of this scenario is the case where the right-handed sleptons of the e and μ type have mass so close to that of the $\tilde{\tau}_R$ that they are effectively stable against chain decays down to the $\tilde{\tau}_R$. Then any one of the three types of sleptons can emerge as the end product of a typical supersymmetric decay chain. The resulting signals can be linear combinations of some of the above scenarios. For additional details on the phenomenology of the co-NLSP's, see Ref. [42].

Let us return to the scenario in which a moderately massive gluino is the LSP. We have noted that this case can arise in both SUGRA models [6] and in non-conventional GMSB models [18]. (It is important to note that in the GMSB case, the gravitino is expected to be much more massive than the gluino and will not enter into the phenomenology.) Supersymmetric events will terminate with the production of at least two gluinos that turn into the lightest R-hadron, most probably the $R^0 = \tilde{g}g$. Since a hadronic calorimeter measures only the R-hadron kinetic energy, events in which the R-hadron is absorbed in the hadronic calorimeter would also have substantial missing energy that would be an increasingly large fraction of the total energy as the gluino mass becomes large. However, since the \tilde{g} does not chain decay, the associated jet production in $\tilde{g}\tilde{g}$ events would be very different from that of mSUGRA-based models. Experimental limits would need to be re-evaluated.

In R-parity violating low-energy SUGRA models, the LSP is unstable. If the RPV-couplings are sufficiently weak, then the LSP will decay outside the detector, and the standard missing energy signal applies. If the LSP decays inside the detector, the phenomenology of RPV-models depends on the identity of the LSP and the branching ratio of possible final state decay products. If the latter includes a neutrino, then the corresponding RPV supersymmetric events would result in missing energy (through neutrino emission) in association with hadron jets and/or leptons. However, other decay chains are possible depending on the relative strengths of λ_L , λ'_L and λ_B [see Eq. (14)]. Other possibilities include decays into charged leptons in association with jets (with no neutrinos), and decays into purely hadronic final states. Clearly, these latter events would contain little or no missing energy. If R-parity violation is present in GMSB models, the RPV decays of the NLSP can easily dominate over the NLSP decay to the gravitino. In this case, the phenomenology of the NLSP resembles that of the LSP of SUGRA-based RPV models.

8.2 Lepton signatures

Once supersymmetric particles are produced at colliders, they do not necessarily decay to the LSP (or NLSP) in one step. The resulting decay chains can be complex, with a number of steps from the initial decay to the final state [50]. Along the way, decays can produce real or virtual W 's, Z 's and sleptons, which then can produce leptons in their subsequent decays. Thus, many models yield large numbers of supersymmetric events characterized by one or more leptons in association with missing energy and with or without hadronic jets.

One signature of particular note is events containing like-sign di-leptons [52]. The origin of such events is associated with the Majorana nature of the gaugino. For example, $\tilde{g}\tilde{g}$ production, followed by gluino decay via

$$\tilde{g} \rightarrow q\bar{q}\tilde{\chi}_1^\pm \rightarrow q\bar{q}\ell^\pm\nu\tilde{\chi}_1^0 \quad (16)$$

can result in like-sign leptons since the \tilde{g} decay leads with equal probability to either ℓ^+ or ℓ^- . If the masses and mass differences are both substantial (which is typical in mSUGRA models, for example), like-sign di-lepton events will be characterized by fairly energetic jets and isolated leptons and by large \cancel{E}_T from the LSP's. Other like-sign di-lepton signatures can arise in a similar way from the decay chains initiated by the heavier neutralinos.

Distinctive tri-lepton signals [53] can result from $\tilde{\chi}_1^\pm\tilde{\chi}_2^0 \rightarrow (\ell^\pm\tilde{\chi}_1^0)(Z^*\tilde{\chi}_1^0)$ when $Z^* \rightarrow \ell^+\ell^-$. Such events have little hadronic activity (apart from initial state radiation of jets off the annihilating quarks at hadron colliders). These events can have a variety of interesting characteristics depending on the fate of the final state neutralinos.

In GMSB models with a charged slepton NLSP, the decay $\tilde{\ell} \rightarrow \ell\tilde{g}_{3/2}$ (if prompt) yields at least two leptons for every supersymmetric event in association with missing energy. In particular, in models with a $\tilde{\tau}_R$ NLSP, supersymmetric events will characteristically contain at least two τ 's.

In RPV models, decays of the LSP (in SUGRA models) or NLSP (in GMSB models) mediated by RPV-interactions proportional to λ_L and λ'_L will also yield supersymmetric events containing charged leptons. However, if the only significant RPV-interaction is the one proportional to λ'_L , then such events would *not* contain missing energy (in contrast to the GMSB signature described above).

8.3 b -quark signatures

The phenomenology of gluinos and squarks depends critically on their relative masses. If gluinos are heavier, they will decay dominantly into $q\tilde{q}$,ⁿ while the squark can decay into quark plus chargino or neutralino. If squarks are heavier, the squarks will decay dominantly into quark plus gluino, while the gluino will decay into the three-body modes $q\tilde{q}\tilde{\chi}$ (where $\tilde{\chi}$ can be either a neutralino or chargino, depending on the charge of the final state quarks). A number of special cases can arise when the possible mass splitting among squarks of different flavors is taken into account. For example, in mSUGRA models it is often the case that the third generation squarks are lighter than the squarks of the first two generations. If the gluino is lighter than the latter but heavier than the former, then the only open gluino two-body decay mode could be $b\tilde{b}$.^o In such a case, all $\tilde{g}\tilde{g}$ events will result in at least four b -quarks in the final state (in association with the usual missing energy signal, if appropriate). The **1**, **24** and **200** Snowmass96 point scenarios of Table 2 yield precisely this situation. The \tilde{g} decay chains in these three scenarios are:

$$\begin{aligned}
\mathbf{1} : \quad & \tilde{g} \xrightarrow{90\%} \tilde{b}_L \bar{b} \xrightarrow{99\%} \tilde{\chi}_2^0 b \bar{b} \xrightarrow{79\%} \tilde{\chi}_1^0 b \bar{b} + (e^+ e^-, \mu^+ \mu^-, \nu \bar{\nu}, q \bar{q}) \\
& \quad \quad \quad \xrightarrow{8\%} \tilde{\chi}_1^0 b \bar{b} + b \bar{b} \\
\mathbf{24} : \quad & \tilde{g} \xrightarrow{85\%} \tilde{b}_L \bar{b} \xrightarrow{70\%} \tilde{\chi}_2^0 b \bar{b} \xrightarrow{99\%} h^0 \tilde{\chi}_1^0 b \bar{b} \xrightarrow{28\%} \tilde{\chi}_1^0 b \bar{b} b \bar{b} \\
& \quad \quad \quad \xrightarrow{69\%} \tilde{\chi}_1^0 \tilde{\chi}_1^0 \tilde{\chi}_1^0 b \bar{b} \\
\mathbf{200} : \quad & \tilde{g} \xrightarrow{99\%} \tilde{b}_L \bar{b} \xrightarrow{100\%} \tilde{\chi}_1^0 b \bar{b}
\end{aligned}$$

More generally, due to the flavor independence of the strong interactions, one expects three-body gluino decays into b -quarks in $\sim 20\%$ of all gluino decays.^p Additional b -quarks can arise from both top-quark and top-squark decays, and from neutral Higgs bosons produced somewhere in the chain decays [54].

These observations suggest that many supersymmetric events at hadron colliders will be characterized by b -jets in association with missing energy [3,55].

ⁿIn this section, we employ the notation $q\tilde{q}$ to mean either $q\tilde{q}$ or $\bar{q}\tilde{q}$.

^oAlthough one top-squark mass-eigenstate (\tilde{t}_1) is typically lighter than \tilde{b} in models, the heavy top-quark mass may result in a kinematically forbidden gluino decay mode into $t\tilde{t}_1$.

^pHere we assume the approximate degeneracy of the first two generations of squarks, as suggested from the absence of FCNC decays. In many models, the b -squarks tend to be of similar mass or lighter than the squarks of the first two generations.

8.4 Signatures involving photons

In mSUGRA models, most supersymmetric events do not contain isolated energetic photons. However, some special regions of low-energy supersymmetric parameter space do exist in which final state photons are probable in the decay chains of supersymmetric particles. For example, if one relaxes the condition of gaugino mass unification [Eq. (4)], and chooses $M_1 \simeq M_2$, then the branching ratio for $\tilde{\chi}_2^0 \rightarrow \tilde{\chi}_1^0 \gamma$ can be significant [56]. In one particular model of this type [5], the $\tilde{\chi}_1^0$ -LSP is dominantly higgsino, while $\tilde{\chi}_2^0$ is dominantly gaugino. Thus, many supersymmetric decay chains end in the production of $\tilde{\chi}_2^0$, which then decays to $\tilde{\chi}_1^0 \gamma$. In this picture, the pair production of supersymmetric particles often yields two photons plus associated missing energy. At LEP-2, one can also produce $\tilde{\chi}_1^0 \tilde{\chi}_2^0$ which would then yield single photon events in association with large missing energy.

In GMSB models with a $\tilde{\chi}_1^0$ -NLSP, all supersymmetric decay chains would end up with the production of $\tilde{\chi}_1^0$. In many models, the branching ratio for $\tilde{\chi}_1^0 \rightarrow \gamma \tilde{g}_{3/2}$ is significant (and could be as high as 100% if other possible two-body decay modes are not kinematically allowed). Assuming that $\tilde{\chi}_1^0$ decays inside the collider detector, supersymmetric pair production would yield events with two photons in association with large missing energy. The characteristics of these events differ in detail from those of the corresponding events expected in the model of Ref. [5].

8.5 Kinks and long-lived particles

In most SUGRA-based models, all heavy sparticles decay promptly in the decay chain until the LSP is reached. The LSP is exactly stable and escapes the collider detector. However, exceptions are possible. In particular, if there is a supersymmetric particle that is just barely heavier than the LSP, then its (three-body) decay rate to the LSP will be significantly suppressed and it could be long lived. For example, in the models with $M_1 > M_2$ [51,6] implying $m_{\tilde{\chi}_1^\pm} \simeq m_{\tilde{\chi}_1^0}$, the $\tilde{\chi}_1^\pm$ can be sufficiently long-lived to yield a detectable vertex, or perhaps even exit the detector.

In GMSB models, the NLSP may be long-lived, depending on its mass and the scale of supersymmetry breaking, \sqrt{F} . The couplings of the NLSP to the helicity $\pm \frac{1}{2}$ components of the gravitino are fixed by Eq. (1), as described earlier. For $\sqrt{F} \sim 100\text{--}10^4$ TeV, this coupling is very weak, implying that all the supersymmetric particles other than the NLSP undergo chain decays down to the NLSP (the branching ratio for the direct decay to the gravitino is negligible). The NLSP is unstable and eventually decays to the gravitino. For example, in the case of the $\tilde{\chi}_1^0$ -NLSP (which is dominated by its U(1)-gaugino

component) one can use Eq. (1) to obtain the decay rate $\Gamma(\tilde{\chi}_1^0 \rightarrow \gamma \tilde{g}_{3/2}) = m_{\tilde{\chi}_1^0}^5 \cos^2 \theta_W / 16\pi F^2$. It then follows that

$$(c\tau)_{\tilde{\chi}_1^0 \rightarrow \gamma \tilde{g}_{3/2}} \sim 130 \left(\frac{100 \text{ GeV}}{m_{\tilde{\chi}_1^0}} \right)^5 \left(\frac{\sqrt{F}}{100 \text{ TeV}} \right)^4 \mu\text{m}. \quad (17)$$

For simplicity, assume that $\tilde{\chi}_1^0 \rightarrow \gamma \tilde{g}_{3/2}$ is the dominant NLSP decay mode. If $\sqrt{F} \sim 3000 \text{ TeV}$ ⁹ then the decay length for the NLSP is $c\tau \sim 100 \text{ m}$ for $m_{\tilde{\chi}_1^0} = 100 \text{ GeV}$; while $\sqrt{F} \sim 100 \text{ TeV}$ implies a short but vertexable decay length.

A similar result is obtained in the case of a charged NLSP. Thus, if \sqrt{F} is sufficiently large, the charged NLSP will be semi-stable and may decay outside of the collider detector.

8.6 Exotic supersymmetric signatures

If R-parity is not conserved, supersymmetric phenomenology exhibits features that are quite distinct from those of the MSSM. Both $\Delta L = 1$ and $\Delta L = 2$ phenomena are allowed (if L is violated), leading to neutrino masses and mixing, neutrinoless double beta decay, and sneutrino-antisneutrino mixing. Further, since the distinction between the Higgs and matter multiplets is lost, R-parity violation permits the mixing of sleptons and Higgs bosons, the mixing of neutrinos and neutralinos, and the mixing of charged leptons and charginos, leading to more complicated mass matrices and mass eigenstates than in the MSSM.

Consequences for collider signatures are numerous. Most important, the LSP is no longer stable, which implies that not all supersymmetric decay chains must yield missing-energy events at colliders. All $\tilde{\chi}_1^0$ decays contain visible particles:

$$\tilde{\chi}_1^0 \rightarrow \underbrace{(3j)}_{\lambda_B \neq 0}, \quad \underbrace{(\ell \ell^{(\prime)} \nu)}_{\lambda_L \neq 0}, \quad \underbrace{(\ell 2j, \nu 2j)}_{\lambda'_L \neq 0}. \quad (18)$$

Thus, even $e^+e^- \rightarrow \tilde{\chi}_1^0 \tilde{\chi}_1^0$ pair production becomes visible. A sneutrino decaying via $\tilde{\nu} \rightarrow \nu \tilde{\chi}_1^0$ also becomes visible. For $\lambda_L \neq 0$, sneutrino resonance production in e^+e^- [57] or $\mu^+\mu^-$ [58] collisions becomes possible. For $\lambda'_L \neq 0$, squarks can be regarded as leptoquarks since the following processes are allowed: $e^+ \bar{u}_m \rightarrow \tilde{d}_n \rightarrow e^+ \bar{u}_m, \bar{\nu} \bar{d}_m$ and $e^+ d_m \rightarrow \tilde{u}_n \rightarrow e^+ d_m$. (Here, m and n are generation labels, so that $d_2 = s, d_3 = b$, etc.) These processes have

⁹Recall that larger values are probably forbidden in order to avoid overclosing the universe.

received much attention during the past year as a possible explanation for the HERA high- Q^2 anomaly [59]. The same term responsible for the processes displayed above could also generate purely hadronic decays for sleptons and sneutrinos: *e.g.*, $\tilde{\ell}_p^- \rightarrow \bar{u}_m d_n$ and $\tilde{\nu}_p \rightarrow \bar{q}_m q_n$ ($q = u$ or d). If such decays were dominant, then the pair production of sleptons in e^+e^- events would lead to hadronic four-jet events with jet pairs of equal mass [60], a signature quite different from the missing energy signals expected in the MSSM. Alternatively, $\lambda_L \neq 0$ could result in substantial branching fractions for $\tilde{\ell} \rightarrow \ell \nu$ and $\tilde{\nu} \rightarrow \ell^+ \ell^-$ decays. Sneutrino pair production would then yield events containing four charged leptons with two lepton pairs of equal mass.

9 Supersymmetry searches at future colliders

In this section, we consider the potential for discovering and studying low-energy supersymmetry at future colliders. Various supersymmetric signatures have been reviewed earlier, and we now apply these to supersymmetry searches at future hadron colliders. Ultimately, the goal of experimental studies of supersymmetry is to measure as many of the MSSM-124 parameters (and any additional parameters that can arise in non-minimal extensions) as possible. In practice, a fully general analysis will be difficult, particularly during the initial supersymmetry discovery phase. Thus, we focus the discussion in this section on the expected phenomenology of supersymmetry at the various future facilities under a number of different model assumptions. Eventually, if candidates for supersymmetric phenomena are discovered, one would plan to utilize precision experimental measurements to map out the supersymmetric parameter space and uncover the structure of the underlying supersymmetry-breaking.

9.1 SUGRA-based models

We begin with the phenomenology of mSUGRA. Of particular importance are the relative sizes of the different supersymmetric particle masses, which are predicted in terms of the mSUGRA parameters. An important generic feature of the resulting superpartner mass spectrum is that substantial phase space is available for most decays occurring in a given chain decay of a heavy supersymmetric particle.

Extensive Monte Carlo studies have determined the region of mSUGRA parameter space for which direct discovery of supersymmetric particles at the Tevatron and the LHC will be possible [61]. At the hadron colliders, the ultimate supersymmetric mass reach is most often determined by the searches for the strongly-interacting superpartners (squarks and gluinos), although at the Tevatron, the tri-lepton signature will be stronger in Run-II and at TeV-33

if $\tan\beta$ is small. Cascade decays then lead to events with jets, missing energy, and/or various numbers of leptons. Gluino and squark masses up to about 400 GeV (or the equivalent in terms of $m_{\tilde{\chi}_1^\pm}, m_{\tilde{\chi}_2^0}$) can be probed at the upcoming Tevatron Run-II; further improvements are projected at the proposed TeV-33 upgrade [62], where supersymmetric masses up to about 600 GeV can be reached. The maximum reach at the LHC is attained by searching in the $1\ell + \text{jets} + \cancel{E}_T$ channel; one will be able to discover squarks and gluinos with masses up to several TeV [63]. Some particularly important classes of events include:

- $pp \rightarrow \tilde{g}\tilde{g} \rightarrow \text{jets} + \cancel{E}_T$ and $\ell^\pm\ell^\pm + \text{jets} + \cancel{E}_T$, (the like-sign dilepton signal [52]).^r For much of parameter space, the mass difference $m_{\tilde{g}} - m_{\tilde{\chi}_1^\pm}$ can be determined from jet spectra end points [52,55,64], while $m_{\tilde{\chi}_1^\pm} - m_{\tilde{\chi}_1^0}$ can be determined from ℓ spectra end points in the like-sign channel [52,55,64]. An absolute scale for $m_{\tilde{g}}$ can be estimated (within an accuracy of roughly $\pm 15\%$) by separating the like-sign events into two hemispheres corresponding to the two \tilde{g} 's [52], by a similar separation in the jets + \cancel{E}_T channel [63], or variations thereof [55,64].
- $pp \rightarrow \tilde{\chi}_1^\pm\tilde{\chi}_2^0 \rightarrow (\ell^\pm\tilde{\chi}_1^0)(Z^*\tilde{\chi}_1^0)$, which yields a trilepton + \cancel{E}_T final state when $Z^* \rightarrow \ell^+\ell^-$; $m_{\tilde{\chi}_2^0} - m_{\tilde{\chi}_1^0}$ is easily determined if enough events are available [53].
- $pp \rightarrow \tilde{\ell}\tilde{\ell} \rightarrow 2\ell + \cancel{E}_T$, detectable at the LHC for $m_{\tilde{\ell}} \lesssim 300$ GeV [63].
- Squarks will be pair produced and, for $m_0 \gg m_{1/2}$, would lead to $\tilde{g}\tilde{g}$ events with two extra jets emerging from the primary $\tilde{q} \rightarrow q\tilde{g}$ decays.

The LHC provides significant opportunities for precision measurements of the mSUGRA parameters [55]. In general, one expects large samples of supersymmetric events with distinguishing features that allow an efficient separation from Standard Model backgrounds. The biggest challenge in analyzing these events may be in distinguishing one set of supersymmetric signals from another. Within the mSUGRA framework, the parameter space is small enough to permit the untangling of the various signals and allows one to extract the mSUGRA parameters with some precision.

Important discovery modes at the eC include the following [65]:

- $e^+e^- \rightarrow \tilde{\chi}_1^+\tilde{\chi}_1^- \rightarrow (q\bar{q}\tilde{\chi}_1^0 \text{ or } \ell\nu\tilde{\chi}_1^0) + (q\bar{q}\tilde{\chi}_1^0 \text{ or } \ell\nu\tilde{\chi}_1^0)$;

^rThe possible predominance of b jets has already been pointed out in Eq. (17).

- $e^+e^- \rightarrow \tilde{\ell}^+\tilde{\ell}^- \rightarrow (\ell^+\tilde{\chi}_1^0 \text{ or } \bar{\nu}\tilde{\chi}_1^+) + (\ell^-\tilde{\chi}_1^0 \text{ or } \nu\tilde{\chi}_1^-).$

In both cases, the masses of the initially produced supersymmetric particles as well as the final state neutralinos and charginos will be well-measured. Here, one is able to make use of the energy spectra end points and beam energy constraints to make precision measurements of masses and determine the underlying supersymmetric parameters. Polarization of the beams is an essential tool that can be used to enhance signals while suppressing Standard Model backgrounds. Moreover, polarization can be employed to separate out various supersymmetric contributions in order to explore the inherent chiral structure of the interactions.

The supersymmetric mass reach is limited by the center-of-mass energy of the eC . For example, if the scalar mass parameter m_0 is too large, squark and slepton pair production will be kinematically forbidden. To probe values of $m_0 \sim 1\text{--}1.5$ TeV requires a collider energy in the range of $\sqrt{s} > 2\text{--}3$ TeV. It could be that such energies will be more easily achieved at a future $\mu^+\mu^-$ collider.

The strength of the lepton colliders lies in their ability to analyze supersymmetric signals and make precision measurements of observables. Ideally, one would like to measure the underlying supersymmetric parameters without prejudice. One could then test the mSUGRA assumptions, and study possible deviations. The most efficient way to carry out such a program is to first use low machine energies to study the light supersymmetric spectrum (lightest charginos and neutralinos and sleptons), and make model-independent measurements of the associated underlying supersymmetric parameters. Once these parameters are ascertained, one can increase the machine energy and analyze with more confidence events with heavy supersymmetric particles decaying via complex decay chains. Thus, the eC and LHC supersymmetric searches are complementary.

Beyond mSUGRA, the MSSM parameter space becomes more complex. As discussed briefly earlier, it is possible to have non-universality among the scalar mass parameters (without generating phenomenologically unacceptable FCNC's) and/or non-universal gaugino masses. We discuss here only a few examples of non-universal gaugino mass scenarios. The first example is the $M_2 < M_1$ possibility, for which the $SU(2)$ -gaugino component is dominant in the lightest chargino and neutralino [51,6]. In this case, the $\tilde{\chi}_1^0$ and $\tilde{\chi}_1^\pm$ can be very degenerate, in which case the visible decay products in the $\tilde{\chi}_1^+ \rightarrow \tilde{\chi}_1^0 \dots$ decays will be very soft and difficult to detect.^s Consequences for chargino and

^sOf course, in the limit of extreme degeneracy, the $\tilde{\chi}_1^+$ will be long lived and be detectable as a visible track in the vertex detector or electromagnetic calorimeter.

neutralino detection in e^+e^- and $\mu^+\mu^-$ collisions, including the importance of the $e^+e^- \rightarrow \gamma\tilde{\chi}_1^+\tilde{\chi}_1^-$ production channel, are discussed in Refs. [51,6]. There is also the possibility that $m_{\tilde{g}} \sim m_{\tilde{\chi}_1^\pm} \simeq m_{\tilde{\chi}_1^0}$. The decay products in the \tilde{g} decay chain would then be very soft, and isolation of $\tilde{g}\tilde{g}$ events would be much more difficult at hadron colliders than in the usual mSUGRA case. In particular, hard jets in association with missing energy would be much rarer, since they would only arise from initial state radiation. The corresponding reduction in supersymmetric parameter space coverage for Run-II at the Tevatron and TeV-33 is explored in Ref. [6].

As a second example, consider the case where the low-energy gaugino mass parameters satisfy $M_2 \sim M_1$.^t If we also assume that $\tan\beta \sim 1$ and $|\mu| < M_1, M_2$,^u then the lightest two neutralinos are nearly a pure photino and higgsino respectively, *i.e.*, $\tilde{\chi}_2^0 \simeq \tilde{\gamma}$ and $\tilde{\chi}_1^0 \simeq \tilde{H}$. For this choice of MSSM parameters, one finds that the rate for the one-loop decay $\tilde{\chi}_2^0 \rightarrow \gamma\tilde{\chi}_1^0$ dominates over all tree level decays of $\tilde{\chi}_2^0$ and $BF(\tilde{e} \rightarrow e\tilde{\chi}_2^0) \gg BF(\tilde{e} \rightarrow e\tilde{\chi}_1^0)$. Clearly, the resulting phenomenology differs substantially from mSUGRA expectations. This scenario was inspired by the CDF $ee\gamma\gamma$ event [44]. Suppose that the $ee\gamma\gamma$ event resulted from $\tilde{e}\tilde{e}$ production, where $\tilde{e} \rightarrow e\tilde{\chi}_2^0 \rightarrow e\gamma\tilde{\chi}_1^0$. Then one would expect a number of other distinctive supersymmetric signals to be observable at LEP-2 (running at its maximal energy) and at Run-II of the Tevatron. In particular, at LEP-2 ($\sqrt{s} = 190$ GeV) with $L = 500$ pb⁻¹ of data one expects more than 50 $\ell\ell + X + \cancel{E}_T$ events and at least 3 $\gamma\gamma + X + \cancel{E}_T$ events. At the Tevatron with $L = 100$ pb⁻¹ of data, one predicts more than 30, 2, 15, 4, 2 and 2 events of the types $\ell\ell + X + \cancel{E}_T$, $\gamma\gamma + X + \cancel{E}_T$, $\ell\gamma + X + \cancel{E}_T$, $\ell\ell\gamma + X + \cancel{E}_T$, $\ell\gamma\gamma + X + \cancel{E}_T$, and $\ell\ell\ell + X + \cancel{E}_T$, respectively. In the above signatures, X stands for additional leptons, photons, and/or jets. These signatures can also arise in GMSB models, although the kinematics of the various events can often be distinguished.

As a final example, we return to the scenario in which the $R^0 = \tilde{g}g$ is the LSP. What would be the signatures at a hadronic accelerator? If m_{R^0} is not large, an initially energetic bare gluino will develop into a hadronic jet containing an R^0 . There will be little apparent missing energy since both the non- R^0 components of the jet and the strongly-interacting R^0 itself would deposit energy in the hadronic calorimeter. Thus, at small m_{R^0} , current limits on $\tilde{g}\tilde{g}$ production at the Tevatron are no longer relevant due to the absence of missing energy. As m_{R^0} increases, the R^0 takes a larger and larger fraction of

^tWe remind the reader that gaugino mass unification at the high-energy scale would predict $M_2 \simeq 2M_1$ [see Eq. (5)].

^uTo achieve such a small μ -parameter requires, *e.g.*, some non-universality among scalar masses of the form $m_{H_d}^2 \neq m_q^2, m_\ell^2$.

the gluino's initial energy and the energy of the R^0 as a fraction of m_{R^0} that appears in the calorimeter becomes smaller and smaller. The maximum energy that can be deposited is the full kinetic energy, $KE = m_{R^0}[1/\sqrt{1-\beta^2} - 1]$. For full deposit of all the KE, the gluino would have to be effectively stopped in the detector. The rest mass energy would then effectively disappear, leading to substantial missing energy. However, from our earlier discussions, it must be remembered that the path length l_p for the R^0 becomes large at large m_{R^0} , so that an R^0 with $m_{R^0} \gtrsim 1$ TeV is likely to simply pass through the detector leaving only a small amount of deposited energy, implying even larger missing energy. Whichever is the case, the Tevatron limits will again fail to apply, not because of an absence of missing energy, but rather because of the small amount of visible energy associated with the gluino-jet — the only visibly energetic jets would be those associated with initial state radiation. For intermediate β values, one could search for delayed energy deposits in the hadronic calorimeter (with an unusual profile associated with the fact that the R^0 would tend to deposit most of its KE at the stopping point). In either case, one could envision searching for the R^0 using a high luminosity, high energy $\sqrt{s} \gtrsim$ several TeV beam dump experiment, in which mass spectrometer or chemical analysis of the dump could be used to search for the R^0 -nuclear isotopes that would be formed. However, if m_{R^0} is above 100 GeV or so, the predicted penetration or stopping length (as discussed earlier) would imply the need for a very large beam dump.

Of course, if squarks are not too heavy, $\tilde{q}\tilde{q}$ production will have substantial rate (if not at the Tevatron, then at the LHC) and each \tilde{q} will decay to $q\tilde{g}$. A heavy \tilde{g} -LSP will yield missing energy as described above and if $m_{\tilde{q}} - m_{\tilde{g}}$ is substantial there will also be significant associated jet activity. Tevatron limits employing the jets plus \cancel{E}_T signal would presumably apply.

9.2 GMSB-based models

The collider signals for GMSB models depend critically on the NLSP identity and its lifetime (or equivalently, its decay length [which depends on the value of \sqrt{F} as shown in Eq. (17)]). In this regard, it should be recalled that values of \sqrt{F} as large as $10^3 - 10^4$ TeV are certainly not disfavored in the GMSB context. Such large values of \sqrt{F} imply very long decay lengths for the NLSP. Thus, we examine the phenomenology of both promptly-decaying and longer-lived NLSP's. In the latter case, the number of decays where one or both NLSP's decay within a radial distance R is proportional to $[1 - \exp(-2R/c\tau)] \simeq 2R/(c\tau)$. For large $c\tau$, most decays would be non-prompt, with many occurring in the outer parts of the detector or completely outside the detector. To maximize

sensitivity to GMSB models and fully cover the (\sqrt{F}, Λ) parameter space, we must develop signals sensitive to decays that are delayed, but not necessarily so delayed as to be beyond current detector coverage and/or specialized extensions of current detectors.

In the discussion below, we focus on various cases, where the NLSP is a neutralino dominated by its U(1)-gaugino (bino) or Higgsino components, and where the NLSP is the lightest charged slepton (usually the $\tilde{\tau}_R$). We first address the case of prompt decays, and then indicate the appropriate strategies for the case of a longer-lived NLSP.

• **Promptly-decaying NLSP: $\tilde{\chi}_1^0 \simeq \tilde{B}$**

We focus on the production of the neutralinos, charginos, and sleptons since these are the lightest of the supersymmetric particles in the GMSB models. The possible decays of the NLSP in this case are: $\tilde{B} \rightarrow \gamma \tilde{g}_{3/2}$ or $\tilde{B} \rightarrow Z \tilde{g}_{3/2}$. The latter is only relevant for the case of a heavier NLSP, and is, in any case, suppressed by a factor of $\tan^2 \theta_W$; it will be ignored in the following discussion.

At hadronic colliders, the $\tilde{\chi}_1^0 \tilde{\chi}_1^0$ production rate is small, but rates for $\tilde{\chi}_1^+ \tilde{\chi}_1^- \rightarrow W^{(*)} W^{(*)} \tilde{\chi}_1^0 \tilde{\chi}_1^0 \rightarrow W^{(*)} W^{(*)} \gamma \gamma + \cancel{E}_T$, $\tilde{\ell}_R \tilde{\ell}_R \rightarrow \ell^+ \ell^- \tilde{\chi}_1^0 \tilde{\chi}_1^0 \rightarrow \ell^+ \ell^- \gamma \gamma + \cancel{E}_T$, $\tilde{\ell}_L \tilde{\ell}_L \rightarrow \ell^+ \ell^- \tilde{\chi}_1^0 \tilde{\chi}_1^0 \rightarrow \ell^+ \ell^- \gamma \gamma + \cancel{E}_T$, *etc.* will all be substantial. Implications for GMSB phenomenology at the Tevatron have been studied in Refs. [43,48,45,16,66]. As noted earlier, it is possible to envision GMSB parameters such that the $ee\gamma\gamma + \cancel{E}_T$ CDF event corresponds to slepton pair production followed by $\tilde{\chi}_1^0 \rightarrow \gamma \tilde{g}_{3/2}$ [43,44,45,46]. However, in this region of GMSB parameter space, other supersymmetric signals should be prevalent, such as $\tilde{\nu}_L \tilde{\ell}_L \rightarrow \ell \gamma \gamma + \cancel{E}_T$ and $\tilde{\nu}_L \tilde{\nu}_L \rightarrow \gamma \gamma + \cancel{E}_T$. The $\tilde{\chi}_2^0 \tilde{\chi}_1^\pm$ and $\tilde{\chi}_1^+ \tilde{\chi}_1^-$ rates would also be significant and lead to $X \gamma \gamma + \cancel{E}_T$ with $X = \ell^\pm, \ell^+ \ell'^-, \ell^+ \ell^- \ell'^\pm$. Limits on these event rates from current CDF and D0 data already eliminate much of the parameter space that could lead to the CDF $ee\gamma\gamma$ event [67].

At LEP-2/eC, the rate for the simplest signal, $e^+ e^- \rightarrow \tilde{\chi}_1^0 \tilde{g}_{3/2} \rightarrow \gamma + \cancel{E}_T$, is expected to be very small [47]. A more robust channel is $e^+ e^- \rightarrow \tilde{\chi}_1^0 \tilde{\chi}_1^0 \rightarrow \gamma \gamma + \cancel{E}_T$ with a (flat) spectrum of photon energies in the range $\frac{1}{4}\sqrt{s}(1 - \beta) \leq E_\gamma \leq \frac{1}{4}\sqrt{s}(1 + \beta)$. Ref. [68] points out that there might be a small excess of such events in the current LEP-2 data, but the level of background requires careful evaluation [69].

• **Promptly decaying NLSP: $\tilde{\chi}_1^0 \simeq \tilde{H}$**

The possible decays of the NLSP in this case are: $\tilde{H} \rightarrow \tilde{g}_{3/2} + h^0, H^0, A^0$, depending on the Higgs masses. If the corresponding two-body decays are not

kinematically possible, then three-body decays (where the corresponding Higgs state is virtual) may become relevant. However, in realistic cases, one expects $\tilde{\chi}_1^0$ to contain small but non-negligible gaugino components, in which case $\tilde{\chi}_1^0 \rightarrow \tilde{g}_{3/2}\gamma$ would dominate all three-body decays. In what follows, we assume that the two-body decay $\tilde{H} \rightarrow \tilde{g}_{3/2}h^0$ is kinematically allowed and dominant. The supersymmetric signals that would emerge at both Tevatron/LHC and LEP-2/eC would then be $4b + X + \cancel{E}_T$ final states, where X represents the decay products emerging from the cascade chain decays of the more massive superparticles. Of course, at LEP-2/eC direct production of higgsino pairs, $e^+e^- \rightarrow \tilde{H}\tilde{H}$ (via virtual s -channel Z -exchange) would be possible in general, leading to pure $4b + \cancel{E}_T$ final states.

• **Promptly decaying NLSP: $\tilde{\ell}_R$**

The dominant slepton decay modes are: $\tilde{\ell}_R^\pm \rightarrow \ell^\pm \tilde{g}_{3/2}$ and $\tilde{\ell}_L^\pm \rightarrow \ell^\pm \tilde{\chi}_1^{0*} \rightarrow \ell^\pm (\tilde{\ell}_R^\pm \ell^\mp)' \rightarrow \ell^\pm (\ell^\pm \ell^\mp)' \tilde{g}_{3/2}$. The $\tilde{\chi}_1^0$ will first decay to $\ell\tilde{\ell}_L$ and $\ell\tilde{\ell}_R$, followed by the above decays.

At both the Tevatron/LHC and LEP-2/eC typical pair production events will end with $\tilde{\ell}_R\tilde{\ell}_R \rightarrow \ell^+\ell^- + \cancel{E}_T$, generally in association with a variety of cascade chain decay products. The lepton energy spectrum will be flat in the $\tilde{\ell}_R\tilde{\ell}_R$ center of mass. Of course, pure $\ell_R\tilde{\ell}_R$ production is possible at LEP/eC and the $\tilde{\ell}_R\tilde{\ell}_R$ center of mass would be the same as the e^+e^- center of mass. Other simple signals at LEP/eC would include $\ell_L\tilde{\ell}_L \rightarrow 6\ell + \cancel{E}_T$.

As noted earlier, if a slepton is the NLSP, it is most likely to be the $\tilde{\tau}_R$. If this state is sufficiently lighter than the \tilde{e}_R and $\tilde{\mu}_R$, then $\tilde{e}_R \rightarrow e\tilde{\tau}_R\tau$ and $\tilde{\mu}_R \rightarrow \mu\tilde{\tau}_R\tau$ decays (via the \tilde{B} component of the mediating virtual neutralino) might dominate over the direct $\tilde{e}_R \rightarrow e\tilde{g}_{3/2}$ and $\tilde{\mu}_R \rightarrow \mu\tilde{g}_{3/2}$ decays and all final states would cascade to τ 's. The relative importance of these different possible decays has been examined in Ref. [70]. A study of this scenario at LEP-2 has been performed in Ref. [49].

• **Longer-lived NLSP: $\tilde{\ell}_R$**

If the $\tilde{\ell}_R$ decays mainly before reaching the electromagnetic calorimeter, then one should look for a charged lepton that suddenly appears a finite distance from the interaction region, with non-zero impact parameter as measured by either the vertex detector or the electromagnetic calorimeter. Leading up to this decay would be a heavily ionizing track with $\beta < 1$ (as could be measured if a magnetic field is present).

If the $\tilde{\ell}_R$ reaches the electromagnetic and hadronic calorimeters, then it behaves much like a heavy muon, presumably interacting in the muon chambers

or exiting the detector if it does not decay first. Limits on such objects should be pursued. Limits are currently quoted by D0 and CDF for pseudo-stable charged strongly produced particles (stable quarks, squarks, . . .), but the rates predicted in GMSB models for $\tilde{\ell}_R$ pairs are very different. There will be many sources of $\tilde{\ell}_R$ production, including direct slepton pair production, and cascade decays resulting from the production of gluinos, squarks, and charginos. A detailed calculation is in progress [71]. Based on the slepton pair cross section at the Tevatron, we estimate that a charged pseudo-stable $\tilde{\ell}_R$ can be ruled out with a mass up to about 80–100 GeV. Similar limits can probably be extracted from LEP-2 data. Including the other production mechanisms should yield a significant extension of the excluded mass range in many GMSB models.

- **Longer-lived NLSP: $\tilde{\chi}_1^0$**

This is a much more difficult case. As before, we assume that the dominant decay of the NLSP in this case is $\tilde{\chi}_1^0 \rightarrow \gamma \tilde{g}_{3/2}$. Clearly, the sensitivity of detectors to delayed γ appearance signals will be of great importance. As noted earlier, if \sqrt{F} is so large that the $\tilde{\chi}_1^0$ escapes the detector before decaying, then the corresponding missing energy signatures are the same as those occurring in SUGRA-based models.

Consider first what is possible at the Tevatron without making use of the delayed γ appearance signals. First, for any magnitude of \sqrt{F} , the jets plus missing energy signal at the Tevatron will only be viable in the limited region of GMSB model parameter space [16] characterized by the GMSB Λ parameter being $\lesssim 30$ TeV ($\lesssim 40$ TeV) in Run-II (at Tev-33); the standard tri-lepton signal will be viable for $\Lambda \lesssim 65$ TeV (75 TeV) [66]. The prompt-two-photon plus missing energy signal deriving from the many sources of prompt $\tilde{\chi}_1^0 \rightarrow \gamma \tilde{g}_{3/2}$ decays discussed earlier is also only visible in a limited portion of parameter space. The regions of viability for Run-II and at Tev-33 are illustrated in Fig. 7. Thus, even after combining the jets-plus-missing-energy, tri-lepton and prompt-two-photon signals, there will be a significant region of (\sqrt{F}, Λ) parameter space that cannot be probed without using the delayed $\tilde{\chi}_1^0 \rightarrow \gamma \tilde{g}_{3/2}$ decays [16,66].

Thus, it is important that the collider detectors develop signals that are sensitive to the delayed $\tilde{\chi}_1^0 \rightarrow \gamma \tilde{g}_{3/2}$ decays. The ability to search for delayed-decay signals is rather critically dependent upon the detector design. The possible signals [16,66] include the following: (a) searching for events where the delayed-decay photon is identified by a large (transverse) impact parameter as it passes into the electromagnetic calorimeter; (b) looking for isolated energy deposits (due to the γ from a delayed $\tilde{\chi}_1^0$ decay) in outer hadronic calorimeter

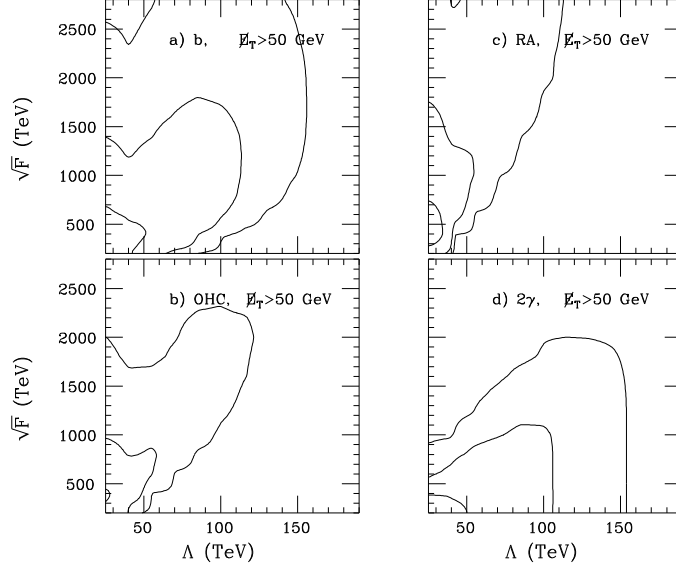


Figure 7: We present cross section contours in the (\sqrt{F}, Λ) parameter space for the (a) impact-parameter (b), (b) outer-hadronic (OHC), (c) roof-array (RA), and (d) prompt-two-photon (2γ) signals. Contours are given at $\sigma = 0.16$ fb (innermost), 2.5 fb (middle), and 50 fb (outermost). Thus, the middle (outermost) contour corresponds to 5 events at Run-II/ $L = 2$ fb $^{-1}$ (TeV-33/ $L = 30$ fb $^{-1}$). In this figure we have taken $E_T^{\text{miss}} = 50$ GeV for all signals.

cells, as possible with the D0 detector; and (c) looking for delayed decays where the $\tilde{\chi}_1^0$ decay occurs outside the main detector and the photon from the decay is observed in a scintillator (or similar device) array placed at a substantial distance from the detector. The observed signal will always contain missing energy from the emitted $\tilde{g}_{3/2}$ or un-decayed $\tilde{\chi}_1^0$, which will be especially useful in reducing potential backgrounds. In all cases, timing information for the detected photon would be extremely valuable. Only if these (or closely related) techniques are employed can one detect GMSB supersymmetry in the bulk (and possibly preferred portion) of parameter space where neither \sqrt{F} nor Λ is small.

A first estimate of the utility of the above signals, is given in Fig. 7, taken from Ref. [66]. In this figure we display cross section contours in the minimal GMSB model for the D0 detector for the three types of signals described above. Cuts have been imposed that should eliminate backgrounds. (A D0 collaboration study is needed for confirmation.) The cuts require a certain number of jets n_j (defined with $\Delta R_{\text{coal}} = 0.5$ and required to have $p_T \geq 25$ GeV and

$|\eta| \leq 3.5$) and one or more delayed photons (required to have $E_\gamma \geq 15$ GeV and be separated from jets by $\Delta R \geq 0.5$) and a minimum amount of missing transverse energy \cancel{E}_T . For all three delayed-decay signals (a), (b) and (c) presented in Fig. 7, we require $n_j \geq 3$ and $\cancel{E}_T \geq 50$ GeV.

(a) The impact parameter (b) signal is defined by requiring that there be one or more $\tilde{\chi}_1^0 \rightarrow \gamma \tilde{g}_{3/2}$ decays in which the impact parameter b of the photon (as measured using the pre-shower and electromagnetic calorimeter) is ≥ 2 cm.^{*v*}

(b) The outer hadronic calorimeter (OHC) signal is defined by requiring that there be one or more $\tilde{\chi}_1^0 \rightarrow \gamma \tilde{g}_{3/2}$ decays in central OHC cells.

(c) The roof array (RA) signal is defined by requiring that there be one or more $\tilde{\chi}_1^0 \rightarrow \gamma \tilde{g}_{3/2}$ decays in which the photon emerges at a vertical height above 6.5 m (*i.e.* outside the detector, in particular, beyond the muon chambers) and passes through a 38 m \times 28 m rectangular detection array centered vertically above the interaction point at a distance of 16.5 m (corresponding to the height of the roof of the D0 detector hall).

Assuming that the backgrounds to all these signals are negligible after our very strong cuts, 5 events will be adequate to claim discovery. Fig. 7 shows that in Run-II (the middle contours) the impact parameter signal will cover almost all of the $\sqrt{F} \lesssim 1500$ TeV and $\Lambda \lesssim 100$ TeV portion of parameter space. The RA and OHC signals would provide important backup and confirmation for the impact parameter signal when $\Lambda \lesssim 50$ TeV. At Tev-33, the regions for which the b , OHC and RA signals are viable expand greatly. In combination, they provide sensitivity to GMSB supersymmetry throughout the preferred $\sqrt{F} \lesssim 3000$ TeV, $\Lambda \lesssim 150$ TeV parameter region for the model examined. Clearly it is of great importance for the D0 and CDF experiments to examine these signals more closely and develop reliable background estimates.

Limits on delayed-decay photon signals from Run-I data ($L \sim 100$ pb⁻¹) require analysis of the OHC signal. A study is underway [72]. The roof array was, of course, not present, and the impact parameter resolution was extremely poor due to the absence of a preshower.

• Gluino-LSP

The phenomenology for this variant [18] of GMSB model would be much as described in the case of a SUGRA model with a gluino-LSP. The primary distinctions would arise from differences in the detailed mass spectra for the heavier sparticles.

^{*v*}Since the expected resolution in b is ~ 0.2 cm, this corresponds to a 10σ excursion from the primary interaction point.

9.3 RPV models

In R-parity violating models, the LSP is no longer stable.^w The relevant signals depend upon the nature of the LSP decay. The phenomenology depends on which R-parity violating couplings [Eq. (14)] are present. For our discussion here, we assume that it is the $\tilde{\chi}_1^0$ that is the LSP, although this is no longer required (by cosmology, *etc.*) if the LSP is not stable.

- At the Tevatron and LHC [73]:

If $\lambda_B \neq 0$, then $\tilde{\chi}_1^0 \rightarrow 3j$ (where $j = \text{jet}$). The large jet backgrounds imply that we would need to rely on the like-sign dilepton signal (which would still be viable despite the absence of missing energy in the events). In general, this signal turns out to be sufficient for supersymmetry discovery out to gluino masses somewhat above 1 TeV. However, if the leptons of the like-sign dilepton signal are very soft, then the discovery reach would be much reduced.^x This is one of the few cases where one could miss discovering low-energy supersymmetry at the LHC. If λ_L dominates $\tilde{\chi}_1^0$ decays, $\tilde{\chi}_1^0 \rightarrow \mu^\pm e^\mp \nu, e^\pm e^\mp \nu$, and there would be many very distinctive multi-lepton signals. If λ'_L is dominant, then $\tilde{\chi}_1^0 \rightarrow \ell jj$ and again there would be distinctive multi-lepton signals.

More generally, many normally invisible signals become visible. An important example is sneutrino pair production. Even if the dominant decay of the sneutrino is $\tilde{\nu} \rightarrow \nu \tilde{\chi}_1^0$ (which is likely if $m_{\tilde{\nu}} > m_{\tilde{\chi}_1^0}$), a visible signal emerges from the $\tilde{\chi}_1^0$ decay as sketched above. Of course, for large enough λ_L or λ'_L the $\tilde{\nu}$'s would have significant branching ratio for decay to lepton pairs or jet pairs, respectively. Indeed, such decays might dominate if $m_{\tilde{\nu}} < m_{\tilde{\chi}_1^0}$.

- At LEP-2, an e^+e^- collider or a $\mu^+\mu^-$ collider:

The simplest process at the lepton colliders is:

$$e^+e^- \rightarrow \tilde{\chi}_1^0 \tilde{\chi}_1^0 \rightarrow \underbrace{(3j)(3j)}_{\lambda_B}, \underbrace{(2\ell\nu)(2\ell\nu)}_{\lambda_L}, \underbrace{(\ell jj)(\ell jj)}_{\lambda'_L} \quad (19)$$

(or the $\mu^+\mu^-$ collision analogue), where the relevant RPV coupling is indicated below the corresponding signal. Substantial rates for equally distinctive signals from production of more massive supersymmetric particles (including sneutrino

^wWe assume that the gravitino is not relevant for phenomenology, as in SUGRA-based models.

^xSoft leptons would occur in models where $m_{\tilde{\chi}_1^\pm} \sim m_{\tilde{\chi}_1^0}$ (which requires non-universal gaugino masses [51,3]).

pair production) would also be present. All these processes (if kinematically allowed) should yield observable supersymmetric signals. Some limits from LEP data already exist [74].

Of particular potential importance for non-zero λ_L is s -channel resonant production of a sneutrino in e^+e^- [57] and $\mu^+\mu^-$ [58] collisions. At a muon collider, this process is detectable down to quite small values of the appropriate λ_L (due to the very excellent beam energy resolution possible at a muon collider), and could be of great importance as a means of actually determining the R-parity-violating couplings. Indeed, for small R-parity-violating couplings, absolute measurements of the couplings through other processes are extremely difficult. This is because such a measurement would typically require the R-parity-violating effects to be competitive with an R-parity-conserving process of known interaction strength. (For example, R-parity-violating neutralino branching ratios constrain only ratios of the R-parity-violating couplings.) Since sneutrino pair production would have been observed at the LHC, an e^+e^- collider and/or the $\mu^+\mu^-$ collider, it would be easy to center on the sneutrino resonance in order to do the crucial sneutrino factory measurements.

- At HERA:

Squark production via R-parity violating couplings could be an explanation for the HERA anomaly at high x and large Q^2 [59]. For example, if $(\lambda'_L)_{113} \sim 0.04\text{--}0.1$, a leptoquark signal from $e^+d_R \rightarrow \tilde{t}_L \rightarrow e^+d$ would be detected if $m_{\tilde{t}_L} \lesssim 220$ GeV.

- Delayed RPV decays:

If the RPV coupling responsible for the decay of the LSP is sufficiently small, but not too small, the LSP decay might not be prompt but could still occur inside the detector or at least not far outside the detector. In this case, the same techniques discussed in the GMSB models for observing delayed $\tilde{\chi}_1^0 \rightarrow \gamma\tilde{g}_{3/2}$ decays could prove very valuable. Delayed $\tilde{\chi}_1^0$ decay OHC energy deposits might occur, leptons $^\nu$ from a delayed $\tilde{\chi}_1^0$ decay might be observed (using the electromagnetic calorimeter and its preshower) to have non-zero impact parameter, and the $\tilde{\chi}_1^0$ could decay outside the detector but before reaching the roof array. Especially at lower energy machines such as the Tevatron, a large extension in parameter space coverage would result from implementing these non-standard detection modes. Further, the relative abundance of events

^yIf the RPV interaction leads to $\tilde{\chi}_1^0 \rightarrow 3j$, then the ability to measure the impact parameters of jets would be important, if possible with sufficient accuracy.

obtained using these different techniques, especially if supplemented with timing information, could allow a determination of the RPV coupling strength. In many scenarios, such determination would not be possible by any other means.

Finally, we note that one should not rule out the possibility that RPV couplings could be present in GMSB models. Unless, the RPV couplings are rather small, the NLSP will decay via the RPV decay channels with a much higher rate than to channels containing the $\tilde{g}_{3/2}$ [75], and all the RPV phenomenology described earlier will apply. However, it is also possible that RPV and $\tilde{g}_{3/2}$ decays of the NLSP will take place at competitive rates. Delayed-decay signals could prove crucial to a full understanding of such a situation.

10 Summary and Conclusions

Low-energy supersymmetry remains the most elegant solution to the naturalness and hierarchy problems, while providing a possible link to Planck scale physics and the unification of particle physics and gravity. Nevertheless, the origin of the soft supersymmetry breaking terms and the details of their structure remain a mystery. There are many theoretical ideas, but we still cannot be certain which region of the MSSM-124 parameter space (or some non-minimal extension thereof) is the one favored by nature. The key theoretical breakthroughs will surely require experimental guidance and input.

Thus, we must rely on our experimental colleagues to uncover evidence for supersymmetry at present or future colliders. Canonical supersymmetric signatures at future colliders are well analyzed and understood. Much of the recent efforts, described in the previous section, have been directed at trying to develop strategies for precision measurements to prove the underlying supersymmetric structure of the interactions and to distinguish among models. However, we are far from understanding all possible facets of MSSM-124 parameter space (even restricted to those regions that are phenomenologically viable). Moreover, the phenomenology of non-minimal and alternative low-energy supersymmetric models (such as models with R-parity violation) and its consequences for collider physics have only recently begun to attract significant attention. The variety of possible non-minimal models of low-energy supersymmetry presents an additional challenge to experimenters who plan on searching for supersymmetry at future colliders.

If supersymmetry is discovered, it will provide a gold mine of experimental signals and theoretical analyses. The many phenomenological manifestations and parameters of supersymmetry suggest that many years of experimental work will be required before it will be possible to determine the precise nature of supersymmetry-breaking and its implications for a more fundamental theory

of particle interactions.

Acknowledgements

This work was supported in part by the Department of Energy and by the Davis Institute for High Energy Physics. I would like to acknowledge the important contributions resulting from collaboration with H.E. Haber on Ref. [1].

References

1. J.F. Gunion and H.E. Haber, UCD-98-1. A cut-down version of this reference will appear in *Perspectives on Supersymmetry*, edited by G. Kane (World Scientific Publishing).
2. M. Olechowski and S. Pokorski, *Phys. Lett.* **B344** (1995) 201.
3. G. Anderson, C.H. Chen, J.F. Gunion, J. Lykken, T. Moroi, Y. Yamada, in *New Directions for High-Energy Physics*, Proceedings of the 1996 DPF/DPB Summer Study on High Energy Physics, Snowmass '96, edited by D.G. Cassel, L.T. Gennari and R.H. Siemann (Stanford Linear Accelerator Center, Stanford, CA, 1997) pp. 669–673.
4. V.S. Kaplunovsky and J. Louis, *Phys. Lett.* **B306** (1993) 269; A. Brignole, L.E. Ibanez and C. Munoz, *Nucl. Phys.* **B422** (1994) 125 [E: **B436** (1995) 747]; CERN-TH/97-143 [hep-ph/9707209].
5. S. Ambrosanio, G.L. Kane, G.D. Kribs, S.P. Martin and S. Mrenna, *Phys. Rev.* **D55** (1997) 1372.
6. C.H. Chen, M. Drees, and J.F. Gunion, *Phys. Rev.* **D55** (1997) 330.
7. G.R. Farrar, *Phys. Rev. Lett.* **76** (1996) 4111, 4115; *Phys. Rev.* **D51** (1995.) 3904 For a recent review, see G.R. Farrar, preprint RU-97-79 [hep-ph/9710277], to appear in the Proceedings of the 5th International Conference on Supersymmetries in Physics (SUSY 97), University of Pennsylvania, Philadelphia, PA, 27–31 May 1997, edited by M. Cvetič and P. Langacker.
8. F. Csikor and Z. Fodor, *Phys. Rev. Lett.* **78** (1997) 4335; preprint ITP-BUDAPEST-538 [hep-ph/9712269]; Z. Nagy and Z. Trocsanyi, hep-ph/9708343; hep-ph/9712385; J. Adams *et al.* [KTeV Collaboration], *Phys. Rev. Lett.* **79** (1997) 4083; P. Abreu *et al.* [DELPHI Collaboration], *Phys. Lett.* **B414** (1997) 401; R. Barate *et al.* [ALEPH Collaboration], *Z. Phys.* **C96** (1997) 1.
9. For a review of gauge-mediated supersymmetry breaking, see G.F. Giudice and R. Rattazzi, CERN-TH/97-380 [hep-ph/9801271], submitted to *Physics Reports*.

10. M.Dine and A.E. Nelson, *Phys. Rev.* **D48** (1993) 1277; M. Dine, A.E. Nelson and Y. Shirman, *Phys. Rev.* **D51** (1995) 1362; M. Dine, A.E. Nelson, Y. Nir and Y. Shirman, *Phys. Rev.* **D53** (1996) 2658.
11. N. Arkani-Hamed, J. March-Russell and H. Murayama, LBL-39865 (1997) [hep-ph/9701286]; H. Murayama, *Phys. Rev. Lett.* **79** (1977) 18; K.-I. Izawa, Y. Nomura, K. Tobe and T. Yanagida, *Phys.Rev.* **D56** (1997) 2886; Y. Nomura and K. Tobe, preprint UT-784 [hep-ph/9708377].
12. S. Martin, *Phys. Rev.* **D55** (1997) 3177.
13. S. Dimopoulos, S. Thomas and J.D. Wells, *Nucl. Phys.* **B488** (1997) 39.
14. J.F. Gunion, UCD-97-9 [hep-ph/9704349], to appear in *Future High Energy Colliders*, proceedings of the ITP Symposium, U.C. Santa Barbara, October 21-25, 1996, AIP Press, ed. Z. Parsa.
15. A. de Gouvea, T. Moroi and H. Murayama, *Phys. Rev.* **D56** (1997) 1281.
16. C.-H. Chen and J.F. Gunion, UCD-97-15 (1997) [hep-ph/9707302].
17. H. Pagels and J.R. Primack, *Phys. Rev. Lett.* **48** (1982) 223; T. Moroi, H. Murayama and M. Yamaguchi, *Phys. Lett.* **B303** (1993) 289; S. Borgani, A. Masiero and M. Yamaguchi, *Phys. Lett.* **B386** (1996) 189.
18. S. Raby, *Phys. Rev.* **D56** (1997) 2852; hep-ph/9712254.
19. G.D. Starkman, A. Gould, R. Esmailzadeh and S. Dimopoulos, *Phys. Rev.* **D41** (1990) 3594.
20. R.N. Mohapatra and S. Nussinov, hep-ph/9708497.
21. For a recent review and guide to the literature, see H. Dreiner, hep-ph/9707435.
22. J.F. Gunion, H.E. Haber, G. Kane, and S. Dawson, *The Higgs Hunter's Guide* (Addison-Wesley Publishing Company, Redwood City, CA, 1990)
23. For a recent review of supersymmetric Higgs boson phenomenology, see J.F. Gunion, hep-ph/9705282, to appear in *Perspectives on Higgs Physics*, ed. G. Kane, 2nd edition (World Scientific Publishing).
24. H.E. Haber and M. Sher, *Phys. Rev.* **D35** (1987) 2206; J. Ellis, J.F. Gunion, H.E. Haber, L. Roszkowski, and F.Zwirner, *Phys. Rev.* **D39** (1989) 844; M. Drees, *Int. J. Mod. Phys.* **A4** (1989) 1989. S.F. King and P.L. White, *Phys. Rev.* **D52** (1995) 4183; **D53** (1996) 4049; U. Ellwanger, M. Rausch de Traubenberg and C.A. Savoy, *Phys. Lett.* **B315** (1993) 331; *Z. Phys.* **C67** (1995) 665; *Nucl. Phys.* **B492** (1997) 21.
25. G.L. Kane, C. Kolda and J.D. Wells, *Phys. Rev. Lett.* **70** (1993) 2686.
26. F. de Campos, M.A. Garcia-Jareno, A.S. Joshipura, J. Rosiek, J.W.F. Valle, *Nucl. Phys.* **B451** (1995) 3; A. Akeroyd, M.A. Diaz, J. Ferrandis, M.A. Garcia-Jareno, J.W.F. Valle, FTUV-97-33 [hep-ph/9707395]; R. Hempfling, in *Neutrinos, Dark Matter and the Universe*, Proceedings of the 8th Rencontres de Blois, 8-13 June 1996, edited by T. Stolar-

- czyk, J. Tran Thanh Van, and F. Vannucci (Editions Frontieres, Gif-sur-Yvette, France, 1997) pp. 381–382; R. Hempfling, preprint UCD-96-36 [hep-ph/9702412].
27. D. Froidevaux, F. Gianotti, L. Poggioli, E. Richter-Was, D. Cavalli, and S. Resconi, ATLAS Internal Note, PHYS-No-74 (1995).
 28. B.R. Kim, S.K. Oh and A. Stephan, *Proceedings of the 2nd International Workshop on “Physics and Experiments with Linear e^+e^- Colliders”*, eds. F. Harris, S. Olsen, S. Pakvasa and X. Tata, Waikoloa, HI (1993), World Scientific Publishing, p. 860; J. Kamoshita, Y. Okada and M. Tanaka, *Phys. Lett.* **B328** (1994) 67.
 29. J.F. Gunion, H.E. Haber and T. Moroi, in *New Directions for High-Energy Physics*, Proceedings of the 1996 DPF/DPB Summer Study on High Energy Physics, Snowmass ’96, edited by D.G. Cassel, L.T. Gennari and R.H. Siemann (Stanford Linear Accelerator Center, Stanford, CA, 1997) pp. 598–602.
 30. V. Barger, M. Berger, J.F. Gunion and T. Han, unpublished.
 31. J.F. Gunion and H.E. Haber, *Phys. Rev.* **D48** (1993) 5109; and in *Research Directions for the Decade*, Proceedings of the 1990 DPF Summer Study on High Energy Physics, Snowmass, CO, 25 June–13 July 1990, edited by E. Berger (World Scientific, Singapore, 1992) p. 469–472.
 32. D. Borden, D. Bauer, and D. Caldwell, *Phys. Rev.* **D48** (1993) 4018.
 33. V. Barger, M. Berger, J. Gunion and T. Han, *Phys. Rev. Lett.* **75** (1995) 1462; hep-ph/9602415, to appear in Physics Reports.
 34. J.F. Gunion and J. Kelly, *Phys. Rev.* **D46** (1997) 1730; a brief summary appears in *New Directions for High-Energy Physics*, Proceedings of the 1996 DPF/DPB Summer Study on High Energy Physics, Snowmass ’96, edited by D.G. Cassel, L.T. Gennari and R.H. Siemann (Stanford Linear Accelerator Center, Stanford, CA, 1997) pp. 632–636.
 35. J. Feng and T. Moroi, *Phys. Rev.* **D56** (1997) 5962.
 36. J.F. Gunion, L. Poggioli, R. Van Kooten, C. Kao and P. Rowson, in *New Directions for High-Energy Physics*, Proceedings of the 1996 DPF/DPB Summer Study on High Energy Physics, Snowmass ’96, edited by D.G. Cassel, L.T. Gennari and R.H. Siemann (Stanford Linear Accelerator Center, Stanford, CA, 1997) pp. 541–587.
 37. J.F. Gunion, UCD-97-17 [hep-ph/9707379], in *Beyond The Standard Model V*, Proceedings of the 5th International Conference, Balholm, Norway, April–May, 1997, edited by G. Eigen, P. Oslan and B. Stugu (American Institute of Physics, Woodbury, NY, 1997) pp. 234–251.
 38. J.F. Gunion, T. Han and R. Sobey, UCD-98-4 [hep-ph/9801317].
 39. J.F. Gunion, B. Grzadkowski, H.E. Haber and J. Kalinowski,

- Phys. Rev. Lett.* **79** (1997) 982.
40. J.F. Gunion, B. Grzadkowski, and X.-G. He, *Phys. Rev. Lett.* **77** (1996) 5172; J.F. Gunion and X.-G. He, UCD-96-23 [hep-ph/9609453], in *New Directions for High-Energy Physics*, Proceedings of the 1996 DPF/DPB Summer Study on High Energy Physics, Snowmass '96, edited by D.G. Cassel, L.T. Gennari and R.H. Siemann (Stanford Linear Accelerator Center, Stanford, CA, 1997) pp. 541–587.
 41. J.F. Gunion and X.-G. He, *Phys. Rev. Lett.* **76** (1996) 4468.
 42. S. Ambrosanio, G.D. Kribs, and S.P. Martin, SLAC-PUB-7668 (1997) [hep-ph/9710217].
 43. See, for example, S. Dimopoulos, S. Thomas and J.D. Wells, *Phys. Rev.* **D54** (1996) 3283; *Nucl. Phys.* **B488** (1997) 39.
 44. S. Ambrosanio, G.L. Kane, G.D. Kribs, S.P. Martin and S. Mrenna, *Phys. Rev.* **D55** (1997) 1372.
 45. S. Ambrosanio, G.L. Kane, G.D. Kribs, S.P. Martin, *Phys. Rev.* **D54** (1996) 5395.
 46. S. Dimopoulos, M. Dine, S. Raby and S. Thomas, *Phys. Rev. Lett.* **76** (1996) 3494; S. Ambrosanio, G.L. Kane, G.D. Kribs, S.P. Martin and S. Mrenna, *Phys. Rev. Lett.* **76** (1996) 3498; J. Ellis, J.L. Lopez and D.V. Nanopoulos, *Phys. Lett.* **B394** (1997) 354.
 47. J. Lopez, D. Nanopoulos and A. Zichichi, *Phys. Rev.* **D55** (1997) 5813, and *Phys. Rev. Lett.* **77** (1996) 5168; S. Dimopoulos, M. Dine, S. Raby and S. Thomas, *Phys. Rev. Lett.* **76** (1996) 3494; S. Ambrosanio, G.D. Kribs and S.P. Martin, *Phys. Rev.* **D56** (1997) 1761; D.R. Stump, M. Wiest and C.-P. Yuan, *Phys. Rev.* **D54** (1996) 1936.
 48. H. Baer, M. Brhlik, C.-H. Chen and X. Tata, *Phys. Rev.* **D55** (1997) 4463;
 49. D.A. Dicus, B. Dutta and S. Nandi, *Phys. Rev. Lett.* **78** (1997) 3055; K. Cheung, D. Dicus, B. Dutta and S. Nandi, UCD-97-24 [hep-ph/9711216].
 50. H. Baer, J. Ellis, G. Gelmini, D. Nanopoulos and X. Tata, *Phys. Lett.* **161B** (1985) 175; G. Gamberini, *Z. Phys.* **C30** (1986) 605; R.M. Barnett, J.F. Gunion and H.E. Haber, *Phys. Rev. Lett.* **60** (1988) 401; *Phys. Rev.* **D37** (1988) 1892; H. Baer, X. Tata and J. Woodside, *Phys. Rev.* **D41** (1990;) 906 *Phys. Rev.* **D45** (1992) 142.
 51. C.H. Chen, M. Drees, and J.F. Gunion, *Phys. Rev. Lett.* **76** (1996) 2002.
 52. R.M. Barnett, J.F. Gunion, and H.E. Haber, *Phys. Lett.* **B315** (1993) 349.
 53. An LHC study is H. Baer, C.H. Chen, F. Paige and X. Tata, *Phys. Rev.* **D50** (1994) 4508. Tevatron studies by theorists include: H. Baer and X. Tata, *Phys. Rev.* **D47** (1993) 2739; H. Baer, C. Kao

- and X. Tata, *Phys. Rev.* **D48** (1993) 5175; J. Lopez, D. Nanopoulos, X. Wang and A. Zichichi, *Phys. Rev.* **D48** (1993) 2062; T. Kamon, J. Lopez, P. McIntyre and J. White, *Phys. Rev.* **D50** (1994) 5676; and H. Baer, C.-H. Chen, R. Munroe, F. Paige and X. Tata, *Phys. Rev.* **D51** (1995) 1046. The most recent SUSY limits based on Tevatron trilepton searches are given in B. Abbott *et al.*, D0 Collaboration, FERMILAB-PUB-97-153-E (1997) [hep-ex/9705015]; and, F. Abe *et al.*, CDF Collaboration, *Phys. Rev. Lett.* **76** (1996) 4307.
54. H. Baer, C.-H. Chen, F.E. Paige and X. Tata, *Phys. Rev.* **D52** (1995) 2746.
 55. I. Hinchliffe, F.E. Paige, M.D. Shapiro, J. Soderqvist and W. Yao, *Phys. Rev.* **D55** (1997) 5520.
 56. H. Komatsu and J. Kubo, *Phys. Lett.* **157B** (1985) 90; *Nucl. Phys.* **B263** (1986) 265; H.E. Haber, G.L. Kane and M. Quiros, *Phys. Lett.* **160B** (1985) 297; *Nucl. Phys.* **B273** (1986) 333; R. Barbieri, G. Gamberini, G.F. Giudice and G. Ridolfi, *Nucl. Phys.* **B296** (1988) 75; H.E. Haber and D. Wyler, *Nucl. Phys.* **B323** (1989.) 267
 57. S. Dimopoulos and L.J. Hall, *Phys. Lett.* **B207** (1988) 210; J. Erler, J.L. Feng and N. Polonsky, *Phys. Rev. Lett.* **78** (1997) 3063.
 58. J.L. Feng, J.F. Gunion and T. Han, UCD-97-25 (1997) [hep-ph/9711414].
 59. D. Choudhury and S. Raychaudhuri, *Phys. Lett.* **B401** (1997) 54; H. Dreiner and P. Morawitz, *Nucl. Phys.* **B503** (1997) 55; G. Altarelli, J. Ellis, G.F. Giudice, S. Lola and M. Mangano, *Nucl. Phys.* **B506** (1997) 3; J. Kalinowski, R. Ruckl, H. Spiesberger and P.M. Zerwas, *Z. Phys.* **C74** (1997) 595; *Phys. Lett.* **B406** (1997) 314; K.S. Babu, C. Kolda, J. March-Russell and F. Wilczek, *Phys. Lett.* **B402** (1997) 367; J. Hewett and T. Rizzo, *Phys. Rev.* **D56** (1997) 5709; SLAC-PUB-7549 [hep-ph/9708419]; For a recent review and further references, see G. Altarelli, CERN-TH/97-195 [hep-ph/9708437], to appear in the Proceedings of the 5th International Conference on Supersymmetries in Physics (SUSY 97), University of Pennsylvania, Philadelphia, PA, 27–31 May 1997, edited by M. Cvetič and P. Langacker.
 60. M. Carena, G.F. Giudice, S. Lola and C.E.M. Wagner, *Phys. Lett.* **B395** (1997) 225.
 61. H. Baer *et al.*, in *Electroweak Symmetry Breaking and New Physics at the TeV Scale*, edited by T.L. Barklow, S. Dawson, H.E. Haber and J.L. Siegrist (World Scientific, Singapore, 1996) pp. 216–291.
 62. See, for example, H. Baer, C.-H. Chen, F. Paige and X. Tata, *Phys. Rev.* **D54** (1996) 5866; D. Amidei *et al.* [TeV-2000 Study Group], FERMILAB-PUB-96-082; and references therein.

63. H. Baer, C.-H. Chen, F. Paige and X. Tata, *Phys. Rev.* **D52** (1995) 2746; *Phys. Rev.* **D53** (1996) 6241.
64. A. Bartl *et al.*, in *New Directions for High-Energy Physics*, Proceedings of the 1996 DPF/DPB Summer Study on High Energy Physics, Snowmass '96, edited by D.G. Cassel, L.T. Gennari and R.H. Siemann (Stanford Linear Accelerator Center, Stanford, CA, 1997) pp. 693–707.
65. T. Tsukamoto, K. Fujii, H. Murayama, M. Yamaguchi and Y. Okada, *Phys. Rev.* **D51** (1995) 3153; H. Baer, R. Munroe and X. Tata, *Phys. Rev.* **D54** (1996) 6735. For a review, see *Physics and Technology of the Next Linear Collider: a Report Submitted to Snowmass 1996*, SLAC Report 485.
66. C.-H. Chen and J.F. Gunion, preprint UCD-97-3.
67. B. Abbott *et al.* [D0 Collaboration] hep-ex/9708005; E. Flattum [for the CDF and D0 Collaborations], FERMILAB-Conf-97/404-E.
68. G.L. Kane, hep-ph/9709318, to appear in the Proceedings of the 5th International Conference on Supersymmetries in Physics (SUSY 97), University of Pennsylvania, Philadelphia, PA, 27–31 May 1997, edited by M. Cvetič and P. Langacker; G.L. Kane and G. Mahlon, *Phys. Lett.* **B408** (1997) 222.
69. S. Mrenna, ANL-HEP-PR-97-27 (1997) [hep-ph/9705441].
70. S. Ambrosanio, G.D. Kribs, S.P. Martin, SLAC-PUB-7668 (1997) [hep-ph/9710217].
71. C.-H. Chen and J.F. Gunion, work in progress.
72. S. Mani *et al.*, D0 collaboration, work in progress.
73. An incomplete set of references is: P. Binetruy and J.F. Gunion, proceedings of the *Workshop on Novel Features of High Energy Hadronic Collisions*, Erice, Italy, 1988, published in *Eloisatron: Heavy Flavors 1988*, p. 489; H. Dreiner, M. Guchait and D.P. Roy, *Phys. Rev.* **D49** (1994) 3270; V. Barger, M.S. Berger, P. Ohmann, R.J.N. Phillips, *Phys. Rev.* **D50** (1994) 4299; H. Baer, C. Kao and X. Tata, *Phys. Rev.* **D51** (1995) 2180; H. Baer, C.-H. Chen and X. Tata, *Phys. Rev.* **D55** (1997) 1466; A. Bartl *et al.*, *Nucl. Phys.* **B502** (1997) 19.
74. Experimental limits from LEP are discussed, for example, in: D. Buskuli *et al.*, ALEPH Collaboration, *Phys. Lett.* **B384** (1996) 461.
75. M. Carena, S. Pokorski, C. Wagner, hep-ph/9801251.